Quantum dynamical entropies in discrete classical chaos

2004 J. Phys. A: Math. Gen. 37 105

(http://iopscience.iop.org/0305-4470/37/1/007)

INSTITUTE OF PHYSICS PUBLISHING JOURNAL OF PHYSICS A: MATHEMATICAL AND GENERAL

J. Phys. A: Math. Gen. **37** (2004) 105–130 PII: S0305-4470(04)67537-8

Quantum dynamical entropies in discrete classical chaos

Fabio Benatti[1,2], **Valerio Cappellini**[1] **and Federico Zertuche**[3]

[1] Dipartimento di Fisica Teorica, Università di Trieste, Strada Costiera 11, 34014 Trieste, Italy
[2] Istituto Nazionale di Fisica Nucleare, Sezione di Trieste, Strada Costiera 11, 34014 Trieste, Italy
[3] Instituto de Matemáticas, UNAM, Unidad Cuernavaca, AP 273-3, Admon. 3, 62251 Cuernavaca, Morelos, Mexico

E-mail: fabio.benatti@ts.infn.it, valerio.cappellini@ts.infn.it and zertuche@matcuer.unam.mx

Received 7 August 2003
Published 10 December 2003
Online at stacks.iop.org/JPhysA/37/105 (DOI: 10.1088/0305-4470/37/1/007)

Abstract

We discuss certain analogies between quantization and discretization of classical systems on manifolds. In particular, we will apply the quantum dynamical entropy of Alicki and Fannes to numerically study the footprints of chaos in discretized versions of hyperbolic maps on the torus.

PACS numbers: 05.45.−a, 05.45.Mt, 89.70.+z

1. Introduction

Classical chaos is associated with motion on a compact phase space with high sensitivity to initial conditions: trajectories diverge exponentially fast and nevertheless remain confined to bounded regions [1–3].

In discrete times, such behaviour is characterized by a positive Lyapounov exponent $\log\lambda, \lambda > 1$ and by a consequent spreading of initial errors δ such that, after n timesteps, $\delta \mapsto \delta_n \simeq \delta\lambda^n$. Exponential amplification on a compact phase space cannot grow indefinitely; therefore, the Lyapounov exponent can only be obtained as

$$\log\lambda := \lim_{t\to\infty} \frac{1}{n} \lim_{\delta\to 0} \log\left(\frac{\delta_n}{\delta}\right)$$

that is by first letting $\delta \to 0$ and only afterwards $n \to \infty$.

In quantum mechanics non-commutativity entails absence of continuous trajectories or, semi-classically, an intrinsic coarse graining of phase space determined by Planck's constant $\hbar$: this forbids δ (the minimal error possible) to go to zero. Thus, if chaotic behaviour is identified with $\log\lambda > 0$, then it is quantally suppressed, unless, performing the classical limit first, we let room for $\delta \to 0$ [4].

In discrete classical systems, one deals with discretized versions of continuous classical systems or with cellular automata [5–7] with a finite number of states. In this case, roughly

speaking, the minimal distance between two states or configurations is strictly larger than zero; therefore, the reason why $\log\lambda$ is trivially zero is very similar to the one encountered in the field of quantum chaos, its origin being now not in non-commutativity but in the lack of a continuous structure. Alternative methods have thus to be developed in order to deal with the granularity of phase space [5–9].

An entropic approach is likely to offer a promising perspective. For sufficiently smooth classical continuous systems, the exponential spreading of errors is equivalent to a net entropy production, better known as Kolmogorov dynamical, or *metric*, entropy [3]. The phase space is partitioned into cells by means of which any trajectory is encoded into a sequence of symbols. As time goes on, the richness in different symbolic trajectories reflects the irregularity of the motion and is associated with strictly positive dynamical entropy [10].

A frequency approach to the numerical evaluation of the entropy production has recently been applied in the discretized version of various chaotic continuous classical dynamical systems [11]. In this paper, we suggest a different strategy: motivated by the similarities between quantization and discretization of continuous classical dynamical systems, we propose to use the quantum dynamical entropy recently introduced by Alicki and Fannes [12, 13], which we shall refer to as ALF-entropy.

The ALF-entropy is based on the algebraic properties of dynamical systems, that is on the fact that, independently of whether they are commutative or not, they are describable by suitable algebras of observables, their time evolution by linear maps on these algebras and their states by expectations over them.

As such, the ALF-entropy applies equally well to classical and quantum systems, and reduces to the Kolmogorov entropy in the former case. In particular, it has been shown that it allows a quite straightforward calculation of the Lyapounov exponents of Arnold cat maps on D-dimensional tori [14].

In this paper we aim at showing how the ALF-entropy may be of use in a discrete classical context, precisely when two-dimensional cat maps are forced to live on a square lattice with spacing $\frac{1}{N}$ (N integer), with particular focus upon the emergence of the continuous behaviour when $N \longmapsto \infty$.

In quantum mechanics, the classical limit is achieved when $\hbar \to 0$. Analogously, in the case of discrete classical systems, by letting the minimal distance between states go to zero, one might hope to recover a well-defined continuous dynamical system, perhaps a chaotic one. Also, very much as in the semi-classical approximation, one expects the possibility of mimicking the behaviour of discrete systems by means of that of their continuous limits and vice versa. However, this is possible only up to a time τ_B, called *breaking-time* [4]; it can be heuristically estimated as the time when the minimal error permitted, δ, becomes of the order of the phase space bound Δ. Therefore, when, in the continuum, a Lyapounov exponent $\log\lambda > 0$ is present, the breaking time scales as $\tau_B = \frac{1}{\log\lambda}\log\frac{\Delta}{\delta}$.

In the following, we shall consider discrete dynamical systems obtained by discretizing a subclass of the unitary modular group of (two-dimensional) toral automorphisms [3] containing the well-known Arnold cat maps. We shall provide

- the algebraic setting for the continuous limit $N \longmapsto \infty$;
- the technical framework to construct the ALF-entropy and numerical shortcuts to compute it;

and study

- the behaviour of the entropy production and how the breaking-time τ_B is reached in hyperbolic systems;
- the differences in behaviour between hyperbolic and elliptic systems;

- the distribution of eigenvalues of the multitime correlation matrix used in computing the ALF-entropy;
- the behaviour of the entropy production in the case of sawtooth maps [15–17] which are discontinuous on the two-dimensional torus.

2. Automorphisms on the torus

Usually, continuous classical motion is described by means of a measure space $\mathcal{X}$, the phase space, endowed with the Borel σ-algebra and a normalized measure μ, $\mu(\mathcal{X}) = 1$. The 'volumes' $\mu(E) = \int_E \mathrm{d}\mu(x)$ of measurable subsets $E \subseteq \mathcal{X}$ represent the probabilities that a phase point $x \in \mathcal{X}$ belongs to them. By specifying the statistical properties of the system, the measure μ defines a 'state' of it.

In such a scheme, a reversible discrete time dynamics amounts to an invertible measurable map $T : \mathcal{X} \mapsto \mathcal{X}$ such that $\mu \circ T = \mu$ and to its iterates $\{T^j\}_{j\in\mathbb{Z}}$. Phase trajectories passing through $x \in \mathcal{X}$ at time 0 are then sequences $\{T^j x\}_{j\in\mathbb{Z}}$ [3].

Classical dynamical systems are thus conveniently described by triplets $(\mathcal{X}, \mu, T)$; in the following, we shall concentrate on triplets $(\mathcal{X}, \mu, T_\alpha)$, where

$$\mathcal{X} = \mathbb{T}^2 = \mathbb{R}^2/\mathbb{Z}^2 = \{\boldsymbol{x} = (x_1, x_2) \pmod 1\} \tag{1a}$$

$$T_\alpha \begin{pmatrix} x_1 \\ x_2 \end{pmatrix} = \begin{pmatrix} 1+\alpha & 1 \\ \alpha & 1 \end{pmatrix} \begin{pmatrix} x_1 \\ x_2 \end{pmatrix} \pmod 1 \qquad \alpha \in \mathbb{Z} \tag{1b}$$

$$\mathrm{d}\mu(\boldsymbol{x}) = \mathrm{d}x_1\, \mathrm{d}x_2. \tag{1c}$$

Remark 2.1.

(i) Since $\det(T_\alpha) = 1$, the Lebesgue measure defined in (1c) is *invariant* for all $\alpha \in \mathbb{Z}$;
(ii) The eigenvalues of $\left(\begin{smallmatrix} 1+\alpha & 1 \\ \alpha & 1 \end{smallmatrix}\right)$ are $\alpha + 2 \pm \sqrt{(\alpha+2)^2 - 4}/2$. They are conjugate complex numbers if $\alpha \in [-4, 0]$, while one eigenvalue λ is greater than 1 if $\alpha \notin [-4, 0]$. In this case, distances are stretched along the direction of the eigenvector $|\boldsymbol{e}_+\rangle$, $S_\alpha|\boldsymbol{e}_+\rangle = \lambda|\boldsymbol{e}_+\rangle$ and contracted along that of $|\boldsymbol{e}_-\rangle$, $S_\alpha|\boldsymbol{e}_-\rangle = \lambda^{-1}|\boldsymbol{e}_-\rangle$. For such α all periodic points are hyperbolic [17].
(iii) $T_1 = \left(\begin{smallmatrix} 2 & 1 \\ 1 & 1 \end{smallmatrix}\right)$ is the Arnold cat map [3]. Then, $T_1 \in \{T_\alpha\}_{\alpha\in\mathbb{Z}} \subset SL_2(\mathbb{T}^2) \subset GL_2(\mathbb{T}^2) \subset ML_2(\mathbb{T}^2)$ where $ML_2(\mathbb{T}^2)$ is the subset of 2×2 matrices with integer entries, $GL_2(\mathbb{T}^2)$ the subset of invertible matrices and $SL_2(\mathbb{T}^2)$ is the subset of matrices with determinant one.
(iv) The dynamics generated by $T_\alpha \in SL_2(\mathbb{T}^2)$ is called the *unitary modular group* [3] (UMG for short).

For future comparison with quantum dynamical systems, we adopt an algebraic point of view and argue in terms of classical observables, precisely in terms of complex continuous functions f on $\mathcal{X} = \mathbb{T}^2$.

- These functions form a C* algebra $\mathcal{A}_\mathcal{X} = \mathcal{C}^0(\mathcal{X})$ with respect to the topology given by the *uniform norm* $\|f\|_0 = \sup_{x\in\mathcal{X}} |f(\boldsymbol{x})|$.
- The Lebesgue measure μ defines a state ω_μ on $\mathcal{A}_\mathcal{X}$ which evaluates mean values of observables via integration:

$$f \mapsto \omega_\mu(f) := \int_\mathcal{X} \mathrm{d}x\, f(x). \tag{2}$$

- The discrete-time dynamics $T_\alpha : \mathcal{X} \mapsto \mathcal{X}$ generates the discrete group of automorphisms $\Theta_\alpha^j : \mathcal{A}_\mathcal{X} \mapsto \mathcal{A}_\mathcal{X}$, given by
$$\Theta_\alpha^j(f)(\boldsymbol{x}) = f\big(S_\alpha^j(\boldsymbol{x})\big) \qquad j \in \mathbb{Z} \tag{3}$$
that preserve the state, $\omega_\mu \circ \Theta_\alpha^j = \omega_\mu$.

Definition 2.1. *The dynamical systems* $(\mathcal{X}, \mu, T_\alpha)$ *will be identified by the algebraic triplets* $(\mathcal{A}_\mathcal{X}, \omega_\mu, \Theta_\alpha)$.

2.1. 'Weyl' discretization

In the following, we shall proceed to a discretization of the systems introduced in the previous section and to the study of how chaos emerges when the continuous limit is being reached.

Roughly speaking, given an integer N, we shall force the continuous classical systems $(\mathcal{A}_\mathcal{X}, \omega_\mu, \Theta_\alpha)$ to live on a lattice $L_N \subset \mathbb{T}^2$ given by
$$L_N := \left\{ \frac{\boldsymbol{p}}{N} \middle| \boldsymbol{p} \in (\mathbb{Z}/N\mathbb{Z})^2 \right\} \tag{4}$$
where $(\mathbb{Z}/N\mathbb{Z})$ denotes the residual class (mod N).

A good indicator of chaos in continuous dynamical systems is the metric entropy of Kolmogorov [3] (see section 3). We can compare discretization of classical continuous systems with quantization; in this way, we can profitably use a quantum extension of the metric entropy which will be presented in section 4. To this aim, we define a discretization procedure resembling Weyl quantization [18, 19]; in practice, we will construct a *morphism $\mathcal{J}_{N,\infty}$ from $\mathcal{A}_\mathcal{X} = \mathcal{C}^0(\mathcal{X})$ into the Abelian algebra $D_{N^2}\mathbb{C}$ of $N^2 \times N^2$ matrices which are diagonal with respect to a chosen orthonormal basis $\{|\boldsymbol{\ell}\rangle\}_{\boldsymbol{\ell}\in(\mathbb{Z}/N\mathbb{Z})^2}$. The basis vectors will be labelled by the points of a square grid of lattice spacing $\frac{1}{N}$ with $0 \leqslant \ell_i \leqslant (N-1)$ (N identified with 0) superimposed onto $\mathcal{X} = \mathbb{T}^2$.

In order to define $\mathcal{J}_{N,\infty}$, we use Fourier analysis and restrict ourselves to the *subalgebra $\mathcal{W}_{\exp} \in \mathcal{A}_\mathcal{X}$ generated by the exponential functions
$$W(\boldsymbol{n})(\boldsymbol{x}) = \exp(2\pi \mathrm{i} \boldsymbol{n}\cdot\boldsymbol{x}) \tag{5}$$
where $\boldsymbol{n} = (n_1, n_2) \in \mathbb{Z}^2$ and $\boldsymbol{n}\cdot\boldsymbol{x} = n_1x_1 + n_2x_2$. The generic element of $\mathcal{W}_{\exp}$ is
$$f(\boldsymbol{x}) = \sum_{\boldsymbol{n}\in\mathbb{Z}^2} \hat{f}_{\boldsymbol{n}} W(\boldsymbol{n})(\boldsymbol{x}) \tag{6}$$
with finitely many coefficients $\hat{f}_{\boldsymbol{n}} = \int\int_\mathcal{X} \mathrm{d}\boldsymbol{x}\, f(\boldsymbol{x})\, \mathrm{e}^{-2\pi \mathrm{i} n x}$ different from zero.

On $\mathcal{W}_{\exp}$, formula (2) defines a state such that
$$\omega_\mu(W(\boldsymbol{n})) = \delta_{\boldsymbol{n},\boldsymbol{0}}. \tag{7}$$
Further, since $\boldsymbol{n}\cdot(T_\alpha\boldsymbol{x}) = \big(T_\alpha^{\mathrm{tr}}\boldsymbol{n}\big)\cdot\boldsymbol{x}$, the automorphisms (3) map exponentials into themselves:
$$\Theta_\alpha(W(\boldsymbol{n})) = W\big(T_\alpha^{\mathrm{tr}}\cdot\boldsymbol{n}\big) \qquad T_\alpha^{\mathrm{tr}} = \begin{pmatrix} 1+\alpha & \alpha \\ 1 & 1 \end{pmatrix}. \tag{8}$$

Remark 2.2. The latter property no longer holds when $\alpha \notin \mathbb{Z}$ as will be the case in section 5.2 where we deal with sawtooth maps [15–17].

Following Weyl quantization, we get elements of D_{N^2} out of elements of $\mathcal{W}_{\exp}$ by replacing, in (6), exponentials with diagonal matrices:
$$W(\boldsymbol{n}) \longmapsto \tilde{W}(\boldsymbol{n}) := \sum_{\boldsymbol{\ell}\in(\mathbb{Z}/N\mathbb{Z})^2} \mathrm{e}^{2\pi \mathrm{i} n\ell/N} |\boldsymbol{\ell}\rangle\langle\boldsymbol{\ell}| \qquad \boldsymbol{\ell} = (\ell_1, \ell_2). \tag{9}$$

Definition 2.2. *We will denote by $\mathcal{J}^{\mathcal{W}}_{N,\infty}$, the *morphism from the *algebra $\mathcal{W}_{\exp}$ into the diagonal matrix algebra $D_{N^2}(\mathbb{C})$, given by*

$$\mathcal{W}_{\exp} \ni f \longmapsto \mathcal{J}^{\mathcal{W}}_{N,\infty}(f) := \sum_{\boldsymbol{n}\in\mathbb{Z}^2} \hat{f}_{\boldsymbol{n}} \tilde{W}(\boldsymbol{n}) = \sum_{\boldsymbol{\ell}\in(\mathbb{Z}/N\mathbb{Z})^2} f\left(\frac{\boldsymbol{\ell}}{N}\right) |\boldsymbol{\ell}\rangle\langle\boldsymbol{\ell}|. \tag{10}$$

Remark 2.3.

(i) The completion of the subalgebra $\mathcal{W}_\infty$ with respect to the uniform norm $\|f\|_0 = \sup_{\boldsymbol{x}\in\mathcal{X}} |f(\boldsymbol{x})|$ is the C* algebra $\mathcal{A}_\mathcal{X} = \mathcal{C}^0(\mathcal{X})$ [20].

(ii) The *morphism $\mathcal{J}^{\mathcal{W}}_{N,\infty} : \mathcal{W}_{\exp} \mapsto D_{N^2}(\mathbb{C})$ is bounded by $\left\|\mathcal{J}^{\mathcal{W}}_{N,\infty}\right\| = 1$. Using the bounded limit theorem [20], $\mathcal{J}^{\mathcal{W}}_{N,\infty}$ can be uniquely extended to a bounded linear transformation (with the same bound) $\mathcal{J}_{N,\infty} : \mathcal{A}_\mathcal{X} \longmapsto D_{N^2}(\mathbb{C})$.

(iii) $\mathcal{J}_{N,\infty}(\mathcal{A}_\mathcal{X}) = D_{N^2}(\mathbb{C})$.

We go back from $D_{N^2}(\mathbb{C})$ to a *algebra of functions on $\mathcal{X}$ by defining a *morphism $\mathcal{J}_{\infty,N}$ that 'inverts' $\mathcal{J}_{N,\infty}$ in the $N \to \infty$ limit. In the Weyl quantization the 'inverting' *morphism is constructed by means of coherent states $|\beta(\boldsymbol{x})\rangle$, $\boldsymbol{x} \in \mathcal{X}$, with good localization properties in $\mathcal{X}$.

Definition 2.3. *We will denote by $\mathcal{J}_{\infty,N} : D_{N^2}(\mathbb{C}) \longmapsto \mathcal{A}_\mathcal{X}$ the *morphism defined by*

$$D_{N^2}(\mathbb{C}) \ni M \longmapsto \mathcal{J}_{\infty,N}(M)(\boldsymbol{x}) := \langle\beta(\boldsymbol{x})|M|\beta(\boldsymbol{x})\rangle \tag{11}$$

where $|\beta(\boldsymbol{x})\rangle$ are coherent vectors in $\mathcal{H}_{N^2} = \mathbb{C}^{N^2}$.

We now construct a suitable family of $|\beta(\boldsymbol{x})\rangle$: we shall denote by $\lfloor\cdot\rfloor$ and $\langle\cdot\rangle$ the integer and fractional parts of a real number so that we can express each $\mathbb{T}^2$ as $\boldsymbol{x} = \left(\frac{\lfloor Nx_1\rfloor}{N}, \frac{\lfloor Nx_2\rfloor}{N}\right) + \left(\frac{\langle Nx_1\rangle}{N}, \frac{\langle Nx_2\rangle}{N}\right)$. Then we associate $\boldsymbol{x} \in \mathbb{T}^2$ with vectors of $\mathcal{H}_{N^2}$ as follows:

$$\begin{aligned}\boldsymbol{x} \mapsto |\beta(\boldsymbol{x})\rangle = {} & \lambda_{11}(\boldsymbol{x})|\lfloor Nx_1\rfloor, \lfloor Nx_2\rfloor\rangle + \lambda_{12}(\boldsymbol{x})|\lfloor Nx_1\rfloor, \lfloor Nx_2\rfloor + 1\rangle \\ & + \lambda_{21}(\boldsymbol{x})|\lfloor Nx_1\rfloor + 1, \lfloor Nx_2\rfloor\rangle + \lambda_{22}(\boldsymbol{x})|\lfloor Nx_1\rfloor + 1, \lfloor Nx_2\rfloor + 1\rangle.\end{aligned} \tag{12}$$

We choose the coefficients λ_{ij} so that $\|\beta(\boldsymbol{x})\| = 1$ and that the map (12) be invertible:

$$\begin{cases} \lambda_{11}(\boldsymbol{x}) = \cos\left(\frac{\pi}{2}\langle Nx_1\rangle\right)\cos\left(\frac{\pi}{2}\langle Nx_2\rangle\right) \\ \lambda_{12}(\boldsymbol{x}) = \cos\left(\frac{\pi}{2}\langle Nx_1\rangle\right)\sin\left(\frac{\pi}{2}\langle Nx_2\rangle\right) \\ \lambda_{21}(\boldsymbol{x}) = \sin\left(\frac{\pi}{2}\langle Nx_1\rangle\right)\cos\left(\frac{\pi}{2}\langle Nx_2\rangle\right) \\ \lambda_{22}(\boldsymbol{x}) = \sin\left(\frac{\pi}{2}\langle Nx_1\rangle\right)\sin\left(\frac{\pi}{2}\langle Nx_2\rangle\right) \end{cases}. \tag{13}$$

Therefore, from definitions 2.2 and 2.3 it follows that, when mapping $\mathcal{A}_\mathcal{X}$ onto $D_{N^2}(\mathbb{C})$ and the latter back into $\mathcal{A}_\mathcal{X}$, we get

$$\begin{aligned}\tilde{f}_N(\boldsymbol{x}) := (\mathcal{J}_{\infty,N} \circ \mathcal{J}_{N,\infty})(f)(\boldsymbol{x}) &= \sum_{\boldsymbol{\ell}\in(\mathbb{Z}/N\mathbb{Z})^2} f\left(\frac{\boldsymbol{\ell}}{N}\right) |\langle\beta(\boldsymbol{x})|\boldsymbol{\ell}\rangle|^2 \\ &= \frac{1}{4} \sum_{(\mu,\nu,\rho,\sigma)\in\{0,1\}^4} \cos(\pi\mu\langle Nx_1\rangle)\cos(\pi\nu\langle Nx_2\rangle)(-1)^{\mu\rho+\nu\sigma} f \\ &\quad \times \left(\frac{\lfloor Nx_1\rfloor + \rho}{N}, \frac{\lfloor Nx_2\rfloor + \sigma}{N}\right).\end{aligned} \tag{14}$$

Remark 2.4.

(i) From (14), $f = \tilde{f}_N$ on the lattice points. Moreover, although the first derivative of (14) is not defined in the latter, its limit exists there and it is zero; thus, we can extend by continuity $\tilde{f}_N$ to a function in $\mathcal{C}1(\mathbb{T}^2)$ that we will denote again as $\tilde{f}_N$.

(ii) We note that $\mathrm{Ran}(\mathcal{J}_{\infty,N})$ is a subalgebra strictly contained in $\mathcal{A}_\mathcal{X}$; this is not surprising and comes as a consequence of Weyl quantization, where this phenomenon is quite typical [18, 19].

We show below that $\mathcal{J}_{\infty,N} \circ \mathcal{J}_{N,\infty}$ approaches $\mathbb{1}_{\mathcal{A}_\mathcal{X}}$ (the identity function in $\mathcal{A}_\mathcal{X}$) when $N \to \infty$. Indeed, a request on any sensible quantization procedure is to recover the classical description in the limit $\hbar \to 0$; in a similar way, our discretization should recover the continuous system in the $\frac{1}{N} \to 0$ limit.

Theorem 1. *Given* $f \in \mathcal{A}_\mathcal{X} = \mathcal{C}^0(\mathbb{T}^2)$, $\lim_{N\to\infty} \left\| \left(\mathcal{J}_{\infty,N} \circ \mathcal{J}_{N,\infty} - \mathbb{1}_{\mathcal{A}_\mathcal{X}}\right)(f) \right\| = 0.$

Proof. Since $\mathcal{X} = \mathbb{T}^2$ is compact, f is uniformly continuous on it. Further, denoting $\boldsymbol{x} = \frac{\lfloor N\boldsymbol{x} \rfloor}{N} + \frac{\langle N\boldsymbol{x} \rangle}{N}$, $0 \leqslant \langle N\boldsymbol{x} \rangle < 1$ implies $\left\| \boldsymbol{x} - \frac{\lfloor N\boldsymbol{x} \rfloor}{N} \right\| \underset{N}{\to} 0$; therefore, for all $\varepsilon > 0$ there exists $N_{f,\varepsilon}$ such that

$$N > \bar{N}_{f,\varepsilon} \Longrightarrow \left| f(\boldsymbol{x}) - f\left(\frac{\lfloor N\boldsymbol{x} \rfloor}{N}\right) \right| < \frac{\varepsilon}{2}$$

uniformly in $\boldsymbol{x}$. Moreover, according to remark 2.4 (i), $\tilde{f}_N \in \mathcal{C}^0(\mathbb{T}^2)$, thus the previous inequality holds for $\tilde{f}_N$, too. Since $\tilde{f}_N = f$ on $\frac{\lfloor N\boldsymbol{x} \rfloor}{N}$, it follows that, for sufficiently large N,

$$|f(\boldsymbol{x}) - \tilde{f}_N(\boldsymbol{x})| \leqslant \left| f(\boldsymbol{x}) - f\left(\frac{\lfloor N\boldsymbol{x} \rfloor}{N}\right) \right| + \left| \tilde{f}_N\left(\frac{\lfloor N\boldsymbol{x} \rfloor}{N}\right) - \tilde{f}_N(\boldsymbol{x}) \right| \leqslant \varepsilon$$

uniformly in $\boldsymbol{x}$. □

3. Kolmogorov metric entropy

For continuous classical systems $(\mathcal{X}, \mu, T_\alpha)$ such as those introduced in section 2, the construction of the dynamical entropy of Kolmogorov is based on subdividing $\mathcal{X}$ into measurable disjoint subsets $\{E_\ell\}_{\ell=1,2,\ldots,D}$ such that $\bigcup_\ell E_\ell = \mathcal{X}$ which form finite partitions (coarse grainings) $\mathcal{E}$.

Under the dynamical maps T_α in (1*b*), any given $\mathcal{E}$ evolves into $T_\alpha^{-j}(\mathcal{E})$ with atoms $T_\alpha^{-j}(E_\ell) = \left\{x \in \mathcal{X} : T_\alpha^j x \in E_\ell\right\}$; one can then form finer partitions $\mathcal{E}_{[0,n-1]}$ whose atoms $E_{i_0 i_1 \cdots i_{n-1}} := E_{i_0} \bigcap T_\alpha^{-1}\left(E_{i_1}\right) \cdots \bigcap T_\alpha^{-n+1}\left(E_{i_{n-1}}\right)$ have volumes

$$\mu_{i_0 i_1 \cdots i_{n-1}} := \mu\left(E_{i_0} \cap T_\alpha^{-1}\left(E_{i_1}\right) \cdots \cap T_\alpha^{-n+1}\left(E_{i_{n-1}}\right)\right). \tag{15}$$

Definition 3.1. *We shall set* $\boldsymbol{i} = \{i_0 i_1 \cdots i_{n-1}\}$ *and denote by* Ω_D^n *the set of* D^n *n-tuples with* i_j *taking values in* $\{1, 2, \ldots, D\}$.

The atoms of the partitions $\mathcal{E}_{[0,n-1]}$ describe segments of trajectories up to time n encoded by the atoms of $\mathcal{E}$ that are traversed at successive times. The richness in diverse trajectories, that is the degree of irregularity of the motion (as seen with the accuracy of the given coarse-graining), can be measured by the Shannon entropy [10]

$$S_\mu(\mathcal{E}_{[0,n-1]}) := -\sum_{\boldsymbol{i} \in \Omega_D^n} \mu_{\boldsymbol{i}} \log \mu_{\boldsymbol{i}}. \tag{16}$$

In the long run, $\mathcal{E}$ attributes to the dynamics an entropy per unit time-step

$$h_\mu(T_\alpha, \mathcal{E}) := \lim_{n\to\infty} \frac{1}{n} S_\mu(\mathcal{E}_{[0,n-1]}). \tag{17}$$

This limit is well defined [3] and the Kolmogorov entropy $h_\mu(T_\alpha)$ of $(\mathcal{A}_\mathcal{X}, \omega_\mu, \Theta_\alpha)$ is defined as the supremum over all finite measurable partitions [3, 10]:

$$h_\mu(T_\alpha) := \sup_{\mathcal{E}} h_\mu(T_\alpha, \mathcal{E}). \tag{18}$$

3.1. Symbolic models as classical spin chains

Finite partitions $\mathcal{E}$ of $\mathcal{X}$ provide symbolic models for the dynamical systems $(\mathcal{X}, \mu, T_\alpha)$ of section 2, whereby the trajectories $\{T_\alpha^j x\}_{j\in\mathbb{Z}}$ are encoded into sequences $\{i_j\}_{j\in\mathbb{Z}}$ of indices relative to the atoms E_{i_j} visited at successive times j; the dynamics corresponds to the right-shift along the symbolic sequences. The encoding can be modelled as the shift along a classical spin chain endowed with a shift-invariant state [12]. This will help to understand the quantum dynamical entropy which will be introduced in the next section.

Let D be the number of atoms of a partition $\mathcal{E}$ of $\mathcal{X}$, we shall denote by $\boldsymbol{A}_D$ the diagonal $D \times D$ matrix algebra generated by the characteristic functions e_{E_ℓ} of the atoms E_ℓ and by $\boldsymbol{A}_D^{[0,n-1]}$ the n-fold tensor product of n copies of $(\boldsymbol{A}_D)$, that is the $D^n \times D^n$ diagonal matrix algebra $\boldsymbol{A}_D^{[0,n-1]} := (\boldsymbol{A}_D)_0 \otimes (\boldsymbol{A}_D)_1 \cdots \otimes (\boldsymbol{A}_D)_{n-1}$. Its typical elements are of the form $a_0 \otimes a_1 \cdots \otimes a_{n-1}$, each a_j being a diagonal $D \times D$ matrix. Every $\boldsymbol{A}_D^{[p,q]} := \otimes_{j=p}^q (\boldsymbol{A}_D)_j$ can be embedded into the infinite tensor product $\boldsymbol{A}_D^\infty := \otimes_{k=0}^\infty (\boldsymbol{A}_D)_k$ as

$$(\mathbb{1})_0 \otimes \cdots \otimes (\mathbb{1})_{p-1} \otimes (\boldsymbol{A}_D)_p \otimes \cdots \otimes (\boldsymbol{A}_D)_q \otimes (\mathbb{1})_{q+1} \otimes (\mathbb{1})_{q+2} \otimes \cdots. \tag{19}$$

The algebra $\boldsymbol{A}_D^\infty$ is a classical spin chain with a classical D-spin at each site.

By means of the discrete probability measure $\{\mu_i\}_{i\in\Omega_D^n}$, one can define a compatible family of states on the 'local' algebras $\boldsymbol{A}_D^{[0,n-1]}$:

$$\rho_\mathcal{E}^{[0,n-1]}(a_0 \otimes \cdots \otimes a_{n-1}) = \sum_{i\in\Omega_D^n} \mu_i (a_0)_{i_0 i_0} \cdots (a_{n-1})_{i_{n-1} i_{n-1}}. \tag{20}$$

Indeed, let $\rho\restriction\boldsymbol{N}$ denote the restriction to a subalgebra $\boldsymbol{N} \subseteq \boldsymbol{M}$ of a state ρ on a larger algebra $\boldsymbol{M}$. Since $\sum_{i_{n-1}} \mu_{i_0 i_1 \cdots i_{n-1}} = \mu_{i_0 i_1 \cdots i_{n-2}}$, when n varies the local states, $\rho_\mathcal{E}^{[0,n-1]}$ are such that $\rho_\mathcal{E}^{[0,n-1]}\restriction\boldsymbol{A}_D^{[0,n-2]} = \rho_\mathcal{E}^{[0,n-2]}$ and define a 'global' state $\rho_\mathcal{E}$ on $\boldsymbol{A}_D^\infty$ such that $\rho_\mathcal{E}\restriction\boldsymbol{A}_D^{[0,n-1]} = \rho_\mathcal{E}^{[0,n-1]}$.

From the T_α-invariance of μ it follows that, under the right-shift $\sigma : \boldsymbol{A}_D^\infty \mapsto \boldsymbol{A}_D^\infty$,

$$\sigma\left(\boldsymbol{A}_D^{[p,q]}\right) = \boldsymbol{A}_D^{[p+1,q+1]} \tag{21}$$

the state $\rho_\mathcal{E}$ of the classical spin chain is translation invariant:

$$\begin{aligned} \rho_\mathcal{E} \circ \sigma(a_0 \otimes \cdots \otimes a_{n-1}) &= \rho_\mathcal{E}\left((\mathbb{1})_0 \otimes (a_0)_1 \otimes \cdots \otimes (a_{n-1})_n\right) \\ &= \rho_\mathcal{E}(a_0 \otimes \cdots \otimes a_{n-1}). \end{aligned} \tag{22}$$

Finally, denoting by $|j\rangle$ the basis vectors of the representation where the matrices $a \in \boldsymbol{A}_D$ are diagonal, local states amount to diagonal density matrices

$$\rho_\mathcal{E}^{[0,n-1]} = \sum_{i\in\Omega_D^n} \mu_i |i_0\rangle\langle i_0| \otimes |i_1\rangle\langle i_1| \otimes \cdots \otimes |i_{n-1}\rangle\langle i_{n-1}| \tag{23}$$

and the Shannon entropy (16) to the von Neumann entropy

$$S_\mu(\mathcal{E}_{[0,n-1]}) = -\operatorname{Tr}\left[\rho_\mathcal{E}^{[0,n-1]} \log \rho_\mathcal{E}^{[0,n-1]}\right] =: H_\mu[\mathcal{E}_{[0,n-1]}]. \tag{24}$$

4. ALF-entropy

From an algebraic point of view, the difference between a triplet $(\mathcal{M}, \omega, \Theta)$ describing a quantum dynamical system and a triplet $\left(\mathcal{A}_{\mathcal{X}}, \omega_{\mu}, \Theta_{\alpha}\right)$ as in definition 2.1 is that ω and Θ are now a Θ-invariant state, respectively, an automorphism over a non-commutative (C* or von Neumann) algebra of operators.

Remark 4.1. In finite dimension D, $\mathcal{M}$ is the full matrix algebra of $D \times D$ matrices, the states ω are given by density matrices ρ_{ω}, such that $\omega(X) := \mathrm{Tr}(\rho_{\omega} X)$, while the reversible dynamics Θ is unitarily implemented: $\Theta(X) = UXU^{*}$.

The quantum dynamical entropy proposed in [12] by Alicki and Fannes, ALF-entropy for short, is based on the idea that, in analogy with what one does for the metric entropy, one can model symbolically the evolution of quantum systems by means of the right-shift along a spin chain. In the quantum case the finite-dimensional matrix algebras at the various sites are not diagonal, but, typically, full matrix algebras, that is the spin at each site is a quantum spin.

This is done by means of the so-called *partitions of unit*, that is by finite sets $\mathcal{Y} = \{y_1, y_2, \ldots, y_D\}$ of operators in a Θ-invariant subalgebra $\mathcal{M}_0 \in \mathcal{M}$ such that

$$\sum_{\ell=1}^{D} y_{\ell}^{*} y_{\ell} = 1 \tag{25}$$

where y_j^{*} denotes the adjoint of y_j. With $\mathcal{Y}$ and the state ω one constructs the $D \times D$ matrix with entries $\omega(y_j^{*} y_i)$; such a matrix is a density matrix $\rho[\mathcal{Y}]$:

$$\rho[\mathcal{Y}]_{i,j} := \omega(y_j^{*} y_i). \tag{26}$$

It is thus possible to define the entropy of a partition of unit as (compare (24))

$$H_{\omega}[\mathcal{Y}] := -\,\mathrm{Tr}(\rho[\mathcal{Y}] \log \rho[\mathcal{Y}]). \tag{27}$$

Further, given two partitions of unit $\mathcal{Y} = (y_0, y_1, \ldots, y_D)$, $\mathcal{Z} = (z_0, z_1, \ldots, z_B)$, of size D, respectively B, one gets a finer partition of unit of size BD as the set

$$\mathcal{Y} \circ \mathcal{Z} := (y_0 z_0, \ldots, y_0 z_B; y_1 z_0, \ldots, y_1 z_B; \ldots; y_D z_0, \ldots, y_D z_B). \tag{28}$$

After j timesteps, $\mathcal{Y}$ evolves into $\Theta^j(\mathcal{Y}) := \{\Theta^j(y_1), \Theta^j(y_2), \ldots, \Theta^j(y_D)\}$. Since Θ is an automorphism, $\Theta^j(\mathcal{Y})$ is a partition of unit; then, one refines $\Theta^j(\mathcal{Y})$, $0 \leqslant j \leqslant n-1$ into a larger partition of unit

$$\mathcal{Y}^{[0,n-1]} := \Theta^{n-1}(\mathcal{Y}) \circ \Theta^{n-2}(\mathcal{Y}) \circ \cdots \circ \Theta(\mathcal{Y}) \circ \mathcal{Y}\,. \tag{29}$$

We shall denote the typical element of $[\mathcal{Y}^{[0,n-1]}]$ by

$$[\mathcal{Y}^{[0,n-1]}]_{\boldsymbol{i}} = \Theta^{n-1}\left(y_{i_{n-1}}\right) \Theta^{n-2}\left(y_{i_{n-2}}\right) \cdots \Theta\left(y_{i_1}\right) y_{i_0}. \tag{30}$$

Each refinement is in turn associated with a density matrix $\rho_{\mathcal{Y}}^{[0,n-1]} := \rho[\mathcal{Y}^{[0,n-1]}]$ which is a state on the algebra $\mathbf{M}_D^{[0,n-1]} := \otimes_{\ell=0}^{n-1}(\mathbf{M}_D)_{\ell}$, with entries

$$[\rho[\mathcal{Y}^{[0,n-1]}]]_{\boldsymbol{i},\boldsymbol{j}} := \omega\left(y_{j_0}^{*} \Theta\left(y_{j_1}^{*}\right) \cdots \Theta^{n-1}\left(y_{j_{n-1}}^{*} y_{i_{n-1}}\right) \cdots \Theta\left(y_{i_1}\right) y_{i_0}\right). \tag{31}$$

Moreover each refinement has an entropy

$$H_{\omega}[\mathcal{Y}^{[0,n-1]}] = -\,\mathrm{Tr}(\rho[\mathcal{Y}^{[0,n-1]}] \log \rho[\mathcal{Y}^{[0,n-1]}]). \tag{32}$$

The states $\rho_{\mathcal{Y}}^{[0,n-1]}$ are compatible: $\rho_{\mathcal{Y}}^{[0,n-1]} \restriction \mathbf{M}_D^{[0,n-2]} = \rho_{\mathcal{Y}}^{[0,n-2]}$, and define a global state $\rho_{\mathcal{Y}}$ on the quantum spin chain $\mathbf{M}_D^{\infty} := \otimes_{\ell=0}^{\infty}(\mathbf{M}_D)_{\ell}$.

Then, as in the previous section, it is possible to associate with the quantum dynamical system $(\mathcal{M}, \omega, \Theta)$ a symbolic dynamics which amounts to the right-shift, $\sigma : (\mathbf{M}_D)_{\ell} \mapsto (\mathbf{M}_D)_{\ell+1}$,

along the quantum spin half-chain (compare (21)). Non-commutativity makes $\rho_{\mathcal{Y}}$ not shift-invariant, in general [12]. In this case, the existence of a limit as in (17) is not guaranteed and one has to define the ALF-entropy of $(\mathcal{M}, \omega, \Theta)$ as

$$h^{\mathrm{ALF}}_{\omega,\mathcal{M}_0}(\Theta) := \sup_{\mathcal{Y}\subset\mathcal{M}_0} h^{\mathrm{ALF}}_{\omega,\mathcal{M}_0}(\Theta, \mathcal{Y}) \tag{33a}$$

where

$$h^{\mathrm{ALF}}_{\omega,\mathcal{M}_0}(\Theta, \mathcal{Y}) := \limsup_n \frac{1}{n} H_\omega[\mathcal{Y}^{[0,n-1]}]. \tag{33b}$$

Like the metric entropy of a partition $\mathcal{E}$, the ALF-entropy of a partition of unit $\mathcal{Y}$ can also be physically interpreted as an asymptotic *entropy production* relative to a specific coarse-graining.

Remark 4.2. The ALF-entropy reduces to the Kolmogorov metric entropy on classical systems. This is best seen by using an algebraic characterization of $(\mathcal{X}, \mu, T_\alpha)$ by means of the von Neumann algebra $\mathcal{M}_{\mathcal{X}} = L^\infty_\mu(\mathcal{X})$ of essentially bounded functions on $\mathcal{X}$ [20]. The characteristic functions of measurable subsets of $\mathcal{X}$ constitute a *subalgebra $\mathcal{M}_0 \subseteq \mathcal{M}_{\mathcal{X}}$; moreover, given a partition $\mathcal{E}$ of $\mathcal{X}$, the characteristic functions e_{E_ℓ} of its atoms E_ℓ, $\mathcal{Z}_{\mathcal{E}} = \{e_{E_1}, \ldots, e_{E_D}\}$ is a partition of unit in $\mathcal{M}_0$. From (3) it follows that $\Theta^j_\alpha(e_{E_\ell}) = e_{T_\alpha^{-j}(E_\ell)}$ and from (2) that $\left[\rho\left[\mathcal{Z}^{[0,n-1]}_{\mathcal{E}}\right]\right]_{i,j} = \delta_{i,j}\mu_i$ (see (15)), whence $H_\omega\left[\mathcal{Z}^{[0,n-1]}_{\mathcal{E}}\right] = S_\mu(\mathcal{E}_{[0,n-1]})$ (see (16) and (27)). In such a case, the lim sup in (33*b*) is actually a true limit and yields (17). In [14], the same result is obtained by means of the algebra $\mathcal{A}_{\mathcal{X}}$ and of the *subalgebra $\mathcal{W}_{\exp}$ of exponential functions.

4.1. ALF-entropy for discretized $(\mathcal{X}, \mu, T_\alpha)$

We now return to the classical systems $(\mathcal{A}_{\mathcal{X}}, \omega_\mu, \Theta_\alpha)$ of section 2. For later use, we introduce the following map defined on the torus $\mathbb{T}^2([0, N)^2)$, namely $[0, N)^2 \pmod N$, and on its subset $(\mathbb{Z}/N\mathbb{Z})^2$:

$$\mathbb{T}^2([0, N)^2) \ni \boldsymbol{x} \mapsto U_\alpha(\boldsymbol{x}) := NT_\alpha\left(\frac{\boldsymbol{x}}{N}\right) \in \mathbb{T}^2([0, N)^2). \tag{34}$$

The use of the *morphisms $\mathcal{J}_{N,\infty}$ and $\mathcal{J}_{\infty,N}$, introduced in section 2.1, makes it convenient to define the discretized versions of $(\mathcal{A}_{\mathcal{X}}, \omega_\mu, \Theta_\alpha)$ as follows:

Definition 4.1. *A discretization of* $(\mathcal{A}_{\mathcal{X}}, \omega_\mu, \Theta_\alpha)$ *is the triplet* $(D_{N^2}(\mathbb{C}), \omega_{N^2}, \tilde{\Theta}_\alpha)$ *where*

- $D_{N^2}(\mathbb{C})$ *is the Abelian algebra of diagonal matrices acting on* $\mathbb{C}^{N^2}$.
- ω_{N^2} *is the tracial state given by the expectation:*

$$D_{N^2}(\mathbb{C}) \ni M \mapsto \omega_{N^2}(M) := \frac{1}{N^2}\,\mathrm{Tr}(M). \tag{35}$$

- $\tilde{\Theta}_\alpha$ *is the* **automorphism of* $D_{N^2}(\mathbb{C})$ *defined by*

$$D_{N^2}(\mathbb{C}) \ni M \mapsto \tilde{\Theta}_\alpha(M) := \sum_{\boldsymbol{\ell}\in(\mathbb{Z}/N\mathbb{Z})^2} M_{U_\alpha(\boldsymbol{\ell}),U_\alpha(\boldsymbol{\ell})}|\boldsymbol{\ell}\rangle\langle\boldsymbol{\ell}|. \tag{36}$$

Remark 4.3.

(i) The expectation $\omega_{N^2}(\mathcal{J}_{N,\infty}(f))$ corresponds to the numerical calculation of the integral of f realized on a $N \times N$ grid on $\mathbb{T}^2$.

(ii) $\tilde{\Theta}_\alpha$ is a *automorphism because the map $(\mathbb{Z}/N\mathbb{Z})^2 \ni \boldsymbol{\ell} \longmapsto U_\alpha(\boldsymbol{\ell})$ is a bijection. For the same reason the state ω_{N^2} is $\tilde{\Theta}_\alpha$-invariant.

(iii) One can check that, given $f \in \mathcal{A}_{\mathcal{X}}$,

$$\tilde{\Theta}_\alpha(\mathcal{J}_{N,\infty}(f)) := \sum_{\ell\in(\mathbb{Z}/N\mathbb{Z})^2} f\left(\frac{U_\alpha(\ell)}{N}\right)|\ell\rangle\langle\ell|. \tag{37}$$

(iv) Also, $\tilde{\Theta}^j_\alpha \circ \mathcal{J}_{N,\infty} = \mathcal{J}_{N,\infty} \circ \Theta^j_\alpha$ for all $j \in \mathbb{Z}$.

(v) In contrast, for $j \in \mathbb{N}$, $\tilde{\Theta}^j_\alpha \circ \mathcal{J}_{N,\infty} \neq \mathcal{J}_{N,\infty} \circ \Theta^j_\alpha$ for the sawtooth maps, that is when $\alpha \notin \mathbb{Z}$.

The automorphism $\tilde{\Theta}_\alpha$ can be rewritten in the more familiar form

$$\begin{aligned}\tilde{\Theta}_\alpha(X) &= \sum_{\ell\in(\mathbb{Z}/N\mathbb{Z})^2} X_{U_\alpha(\ell),U_\alpha(\ell)}|\ell\rangle\langle\ell| \\ &= \sum_{U_\alpha^{-1}(s)\in(\mathbb{Z}/N\mathbb{Z})^2} X_{s,s}\left|U_\alpha^{-1}(s)\right\rangle\left\langle U_\alpha^{-1}s\right| \\ \text{(see remark 4.4, (i) and (ii))} \quad &= U_{\alpha,N}\left(\sum_{\substack{\text{all equiv.}\\ \text{classes}}} X_{s,s}|s\rangle\langle s|\right)U^*_{\alpha,N} \qquad (38)\\ &= U_{\alpha,N}XU^*_{\alpha,N} \qquad (39)\end{aligned}$$

where the operators $U_{\alpha,N}$ are defined by

$$\mathcal{H}_{N^2} \ni |\ell\rangle \longmapsto U_{\alpha,N}|\ell\rangle := \left|\, U_\alpha^{-1}(\ell)\right\rangle. \tag{40}$$

Remark 4.4.

(i) All of T_α, T_α^{-1}, T_α^t and $\left(T_\alpha^{-1}\right)^t$ belong to $SL_2(\mathbb{Z}/N\mathbb{Z})$; in particular these matrices are automorphisms on $(\mathbb{Z}/N\mathbb{Z})^2$ so that, in (38), one can sum over the equivalence classes.

(ii) The same argument as before proves that the operators in (40) are unitary which is equivalent to saying that $\tilde{\Theta}_\alpha$ is a *automorphism.

In order to construct the ALF-entropy, we now seek a useful partition of unit in $(D_{N^2}, \omega_{N^2}, \tilde{\Theta}_\alpha)$; we do that by means of the subalgebra $\mathcal{W}_\infty \subseteq \mathcal{A}_{\mathcal{X}}$ in equations (5) and (6):

$$\mathcal{Y} := \{y_j\}_{j=1}^D = \left\{\frac{1}{\sqrt{D}}\exp(2\pi\mathrm{i}\boldsymbol{r}_j\cdot\boldsymbol{x})\right\}_{j=1}^D \tag{41}$$

where

$$\{\boldsymbol{r}_j\}_{j=1}^D =: \Lambda \subset (\mathbb{Z}/N\mathbb{Z})^2. \tag{42}$$

Definition 4.2. *Given a subset Λ of the lattice consisting of the points $\{\boldsymbol{r}_j\}$ as in (42), we shall denote by $\tilde{\mathcal{Y}}$ the partition of unit in $(D_{N^2}, \omega_{N^2}, \tilde{\Theta}_\alpha)$ given by*

$$\tilde{\mathcal{Y}} = \{\tilde{y}_j\}_{j=1}^D := \{\mathcal{J}_{N,\infty}(y_j)\}_{j=1}^D = \left\{\frac{1}{\sqrt{D}}\tilde{W}(\boldsymbol{r}_j)\right\}_{j=1}^D \tag{43}$$

with $\tilde{W}(\boldsymbol{r}_j)$ defined in (9).

From the above definition, the elements of the refined partitions in (30) take the form

$$[\tilde{\mathcal{Y}}^{[0,n-1]}]_i = \frac{1}{N}\frac{1}{D^{\frac{n}{2}}}\sum_{\ell\in(\mathbb{Z}/N\mathbb{Z})^2}\exp\left(\frac{2\pi\mathrm{i}}{N}\left[\boldsymbol{r}_{i_{n-1}}\cdot U_\alpha^{n-1}(\ell)+\cdots+\boldsymbol{r}_{i_1}\cdot U_\alpha(\ell)+\boldsymbol{r}_{i_0}\cdot\ell\right]\right)|\ell\rangle\langle\ell|. \tag{44}$$

Then, the multitime correlation matrix $\rho_{\tilde{\mathcal{Y}}}^{[0,n-1]}$ in (31) has entries

$$[\rho[\tilde{\mathcal{Y}}^{[0,n-1]}]]_{\boldsymbol{i},\boldsymbol{j}} = \frac{1}{N^2}\frac{1}{D^n}\sum_{\boldsymbol{\ell}\in(\mathbb{Z}/N\mathbb{Z})^2}\exp\left(\frac{2\pi\,\mathrm{i}}{N}\sum_{p=0}^{n-1}\left(\boldsymbol{r}_{i_p}-\boldsymbol{r}_{j_p}\right)\cdot U_\alpha^p(\boldsymbol{\ell})\right)\qquad U_\alpha^0(\boldsymbol{\ell})=1 \tag{45}$$

$$= \sum_{\boldsymbol{\ell}\in(\mathbb{Z}/N\mathbb{Z})^2}\langle \boldsymbol{i}|g_{\boldsymbol{\ell}}(n)\rangle\langle g_{\boldsymbol{\ell}}(n)|\boldsymbol{j}\rangle \tag{46}$$

with

$$\langle \boldsymbol{i}|g_{\boldsymbol{\ell}}(n)\rangle := \frac{1}{N}\frac{1}{D^{\frac{n}{2}}}\exp\left(\frac{2\pi\,\mathrm{i}}{N}\sum_{p=0}^{n-1}\boldsymbol{r}_{i_p}\cdot U_\alpha^p(\boldsymbol{\ell})\right)\in\mathbb{C}^{D^n}. \tag{47}$$

The density matrix $\rho_{\tilde{\mathcal{Y}}}^{[0,n-1]}$ can now be used to numerically compute the ALF-entropy as in (33); however, the large dimension ($D^n\times D^n$) makes the computational problem very hard, a part for small numbers of iterations. Our goal is to prove that another matrix (of fixed dimension $N^2\times N^2$) can be used instead of $\rho_{\tilde{\mathcal{Y}}}^{[0,n-1]}$.

Proposition 4.1. *Let $\mathcal{G}(n)$ be the $N^2\times N^2$ matrix with entries*

$$\mathcal{G}_{\boldsymbol{\ell}_1,\boldsymbol{\ell}_2}(n) := \left\langle g_{\boldsymbol{\ell}_2}(n)\middle|\, g_{\boldsymbol{\ell}_1}(n)\right\rangle \tag{48}$$

given by the scalar products of the vectors $|\,g_{\boldsymbol{\ell}}(n)\,\rangle\in\mathcal{H}_{D^n}=\mathbb{C}^{D^n}$ in (47). Then, the entropy of the partition of unit $\tilde{\mathcal{Y}}^{[0,n-1]}$ with elements (43) is given by

$$H_{\omega_{N^2}}\left[\tilde{\mathcal{Y}}^{[0,n-1]}\right] = -\mathrm{Tr}_{\mathcal{H}_{N^2}}(\mathcal{G}(n)\log\mathcal{G}(n)). \tag{49}$$

Proof. $\mathcal{G}(n)$ is Hermitian and from (47) it follows that $\mathrm{Tr}_{\mathcal{H}_{N^2}}\mathcal{G}(n)=1$.

Let $\mathcal{H}_{N^2}=\mathbb{C}^{N^2}$, $\mathcal{H}:=\mathcal{H}_{D^n}\otimes\mathcal{H}_{N^2}$ and consider the projection $\rho_\psi=|\psi\rangle\langle\psi|$ onto

$$\mathcal{H}\ni|\psi\rangle := \sum_{\boldsymbol{\ell}\in(\mathbb{Z}/N\mathbb{Z})^2}|\,g_{\boldsymbol{\ell}}(n)\rangle\otimes|\,\boldsymbol{\ell}\,\rangle\,. \tag{50}$$

We denote by Σ_1 the restriction of ρ_ψ to the full matrix algebra $M_1:=M_{D^n}(\mathbb{C})$ and by Σ_2 the restriction to $M_2:=M_{N^2}(\mathbb{C})$. It follows that

$$\mathrm{Tr}_{\mathcal{H}_{D^n}}(\Sigma_1\cdot m_1)=\langle\,\psi\,|\,m_1\otimes\mathbb{1}_2|\psi\,\rangle=\sum_{\boldsymbol{\ell}\in(\mathbb{Z}/N\mathbb{Z})^2}\langle\,g_{\boldsymbol{\ell}}\,|\,m_1\,|\,g_{\boldsymbol{\ell}}\,\rangle\qquad\forall m_1\in M_1.$$

Thus, from (46),

$$\Sigma_1=\rho_{\tilde{\mathcal{Y}}}^{[0,n-1]}=\sum_{\boldsymbol{\ell}\in(\mathbb{Z}/N\mathbb{Z})^2}|g_{\boldsymbol{\ell}}(n)\rangle\langle g_{\boldsymbol{\ell}}(n)|. \tag{51}$$

On the other hand, from

$$\mathrm{Tr}_{\mathcal{H}_{N^2}}(\Sigma_2\cdot m_2)=\langle\psi|\mathbb{1}_1\otimes m_2|\psi\rangle$$
$$=\sum_{\boldsymbol{\ell}_1,\boldsymbol{\ell}_2\in(\mathbb{Z}/N\mathbb{Z})^2}\left\langle g_{\boldsymbol{\ell}_2}(n)\middle|\, g_{\boldsymbol{\ell}_1}(n)\right\rangle\langle\boldsymbol{\ell}_2|m_2|\boldsymbol{\ell}_1\rangle\qquad\forall m_2\in M_2$$

it turns out that $\Sigma_2=\mathcal{G}(n)$, whence the result follows from Araki–Lieb's inequality [21]. □

We now return to the explicit computation of the density matrix $\mathcal{G}(n)$ in proposition 4.1. By using the transposed matrix T_α^{tr}, the vectors (47) now read

$$\langle \boldsymbol{i}|g_{\boldsymbol{\ell}}(n)\rangle = \frac{1}{ND^{\frac{n}{2}}}\exp\left(\frac{2\pi\,\mathrm{i}}{N}\boldsymbol{\ell}\cdot\boldsymbol{f}_{\Lambda,\alpha}^{(n),N}(\boldsymbol{i})\right) \tag{52}$$

$$\boldsymbol{f}^{(n),N}_{\Lambda,\alpha}(\boldsymbol{i}) := \sum_{p=0}^{n-1} \left(T^{\mathrm{tr}}_{\alpha}\right)^{p} \boldsymbol{r}_{i_p} \qquad (\mathrm{mod}\ N) \tag{53}$$

where we made explicit the various dependences of (53) on n the time-step, N the inverse lattice spacing, the chosen set Λ of $\boldsymbol{r}_j$ and the α parameter of the dynamics in $SL_2(\mathbb{Z}/N\mathbb{Z})^2$.

In the following we shall use the equivalence classes

$$[\boldsymbol{r}] := \left\{ \boldsymbol{i} \in \Omega^{(n)}_D \middle| \boldsymbol{f}^{(n),N}_{\Lambda,\alpha}(\boldsymbol{i}) \equiv \boldsymbol{r} \in (\mathbb{Z}/N\mathbb{Z})^2 \pmod{N} \right\} \tag{54}$$

their cardinalities $\#[\boldsymbol{r}]$ and, in particular, the frequency function $\nu^{(n),N}_{\Lambda,\alpha}$

$$(\mathbb{Z}/N\mathbb{Z})^2 \ni \boldsymbol{r} \longmapsto \nu^{(n),N}_{\Lambda,\alpha}(\boldsymbol{r}) := \frac{\#[\boldsymbol{r}]}{D^n}. \tag{55}$$

Proposition 4.2. *The von Neumann entropy of the refined (exponential) partition of unit up to time $n-1$ is given by*

$$H_{\omega_{N^2}}[\tilde{\mathcal{Y}}^{[0,n-1]}] = -\sum_{\boldsymbol{r}\in(\mathbb{Z}/N\mathbb{Z})^2} \nu^{(n),N}_{\Lambda,\alpha}(\boldsymbol{r}) \log \nu^{(n),N}_{\Lambda,\alpha}(\boldsymbol{r}). \tag{56}$$

Proof. Using (52), the matrix $\mathcal{G}(n)$ in proposition 4.1 can be written as

$$\mathcal{G}(n) = \frac{1}{D^n} \sum_{\boldsymbol{i}\in\Omega^n_D} |f_{\boldsymbol{i}}(n)\rangle\langle f_{\boldsymbol{i}}(n)| \tag{57}$$

$$\langle \boldsymbol{\ell}|f_{\boldsymbol{i}}(n)\rangle = \frac{1}{N} \exp\left(\frac{2\pi \mathrm{i}}{N} \boldsymbol{f}^{(n),N}_{\Lambda,\alpha}(\boldsymbol{i}) \cdot \boldsymbol{\ell}\right). \tag{58}$$

The vectors $|f_{\boldsymbol{i}}(n)\rangle \in \mathcal{H}_{N^2} = \mathbb{C}^{N^2}$ are such that $\langle f_{\boldsymbol{i}}(n)|f_{\boldsymbol{j}}(n)\rangle = \delta^{(N)}_{\boldsymbol{f}^{(n),N}_{\Lambda,\alpha}(\boldsymbol{i}),\boldsymbol{f}^{(n),N}_{\Lambda,\alpha}(\boldsymbol{j})}$, where $\delta^{(N)}$ is the N-periodic Kronecker delta. For the sake of simplicity, we say that $|f_{\boldsymbol{i}}(n)\rangle$ belongs to the equivalence class $[\boldsymbol{r}]$ in (54) if $\boldsymbol{i} \in [\boldsymbol{r}]$; vectors in different equivalence classes are thus orthogonal, whereas those in the same equivalence class $[\boldsymbol{r}]$ are such that

$$\begin{aligned}\langle \boldsymbol{\ell}_1| \left(\sum_{\boldsymbol{i}\in[\boldsymbol{r}]} |f_{\boldsymbol{i}}(n)\rangle\langle f_{\boldsymbol{i}}(n)|\right) |\boldsymbol{\ell}_2\rangle &= \frac{1}{N^2} \sum_{\boldsymbol{i}\in[\boldsymbol{r}]} \exp\left(\frac{2\pi \mathrm{i}}{N} \boldsymbol{f}^{(n),N}_{\Lambda,\alpha}(\boldsymbol{i}) \cdot (\boldsymbol{\ell}_1 - \boldsymbol{\ell}_2)\right) \\ &= D^n \nu^{(n),N}_{\Lambda,\alpha}(\boldsymbol{r}) \langle \boldsymbol{\ell}_1|\boldsymbol{e}(\boldsymbol{r})\rangle\langle \boldsymbol{e}(\boldsymbol{r})|\boldsymbol{\ell}_2\rangle\end{aligned}$$

$$\langle \boldsymbol{\ell}|\,\boldsymbol{e}(\boldsymbol{r})\rangle = \frac{\exp\left(\frac{2\pi \mathrm{i}}{N} \boldsymbol{r}\cdot\boldsymbol{\ell}\right)}{N} \in \mathcal{H}_{N^2}.$$

Therefore, the result follows from the spectral decomposition

$$\mathcal{G}(n) = \sum_{\boldsymbol{r}\in(\mathbb{Z}/N\mathbb{Z})^2} \nu^{(n),N}_{\Lambda,\alpha}(\boldsymbol{r}) |\boldsymbol{e}(\boldsymbol{r})\rangle\langle \boldsymbol{e}(\boldsymbol{r})|. \qquad \square$$

5. Analysis of entropy production

In agreement with the intuition that finitely many states cannot sustain any lasting entropy production, the ALF-entropy is indeed zero for such systems [12]. However, this does not mean that the dynamics may not be able to show a significant entropy rate over finite intervals of time, these being typical of the underlying dynamics.

As already observed in the introduction, in quantum chaos one deals with quantized classically chaotic systems; there, one finds that classical and quantum mechanics are both correct descriptions over times scaling with $\log \hbar^{-1}$. Therefore, the classical–quantum correspondence occurs over times much smaller than the Heisenberg recursion time that typically scales as $\hbar^{-\alpha}$, $\alpha > 0$. In other words, for quantized classically chaotic systems, the classical description has to be replaced by the quantum one much sooner than for integrable systems.

In this paper, we are considering not the quantization of classical systems, but their discretization; nevertheless, we have seen that, in certain respects, quantization and discretization are similar procedures with the inverse of the number of states N playing the role of $\hbar$ in the latter case.

We are then interested in studying how the classical continuous behaviour emerges from the discretized one when $N \to \infty$; in particular, we want to investigate the presence of characteristic time scales and of 'breaking-times' τ_B, namely those times beyond which the discretized systems cease to produce entropy because their granularity takes over and the dynamics reveals in full its regularity.

Propositions 4.1 and 4.2 afford useful means to attack such a problem numerically. In the following, we shall be concerned with the time behaviour of the entropy of partition of units as in definition 4.2, the presence of breaking-times $\tau_B(\Lambda, N, \alpha)$, and their dependence on the set Λ, on the number of states N and on the dynamical parameter α.

As we shall see, in many cases τ_B depends quite heavily on the chosen partition of unit; we shall then try to cook up a strategy to find a τ_B as stable as possible upon variation of partitions, being led by the idea that the 'true' τ_B has to be strongly related to the Lyapounov exponent of the underlying continuous dynamical system.

Equations (49) and (56) allow us to compute the von Neumann entropy of the state $\rho_{\tilde{\mathcal{Y}}}^{[0,n-1]}$; if we were to compute the ALF-entropy according to the definitions (33), the result would be zero, in agreement with the fact that the Lyapounov exponent for a system with a finite number of states vanishes. Indeed, it is sufficient to note that the entropy $H_{\omega_{N^2}}[\tilde{\mathcal{Y}}^{[0,n-1]}]$ is bounded from above by the entropy of the tracial state $\frac{1}{N^2}\mathbb{1}_{N^2}$, that is by $2\log N$; therefore the expression

$$h_{\omega_{N^2},\mathcal{W}_\infty}(\alpha, \Lambda, n) := \frac{1}{n} H_{\omega_{N^2}}[\tilde{\mathcal{Y}}^{[0,n-1]}] \tag{59}$$

goes to zero with $n \longrightarrow 0$. It is for this reason that, in the following, we will focus on the temporal evolution of the function $h_{\omega_{N^2},\mathcal{W}_\infty}(\alpha, \Lambda, n)$ instead of taking its lim sup over the number of iterations n.

In the same spirit, we will not take the supremum of (59) over all possible partitions $\tilde{\mathcal{Y}}$ (originated by different Λ); instead, we will study the dependence of $h_{\omega_{N^2},\mathcal{W}_\infty}(\alpha, \Lambda, n)$ on different choices of partitions. In fact, if we vary over all possible choices of partitions of unit, we could choose $\Lambda = (\mathbb{Z}/N\mathbb{Z})^2$ in (42), that is $D = N^2$; then summation over all possible $\boldsymbol{r} \in (\mathbb{Z}/N\mathbb{Z})^2$ would make the matrix elements $\mathcal{G}_{\ell_1,\ell_2}(n)$ in (48) equal to $\frac{\delta_{\ell_1,\ell_2}}{N^2}$, whence $H_{\omega_{N^2}}[\tilde{\mathcal{Y}}^{[0,n-1]}] = 2\log N$.

5.1. The case of $T_\alpha \in GL_2(\mathbb{T}^2)$

The maximum of $H_{\omega_{N^2}}$ is reached when the frequencies (55)

$$\nu_{\Lambda,\alpha}^{(n),N} : (\mathbb{Z}/N\mathbb{Z})^2 \mapsto [0, 1]$$

become equal to $1/N^2$ over the torus: we will see that this is indeed what happens to the frequencies $\nu^{(n),N}_{\Lambda,\alpha}$ with $n \longrightarrow \infty$. The latter behaviour can be reached in various ways depending on

- hyperbolic or elliptic regimes, namely on the dynamical parameter α;
- number of elements (D) in the partition Λ;
- mutual location of the D elements $\boldsymbol{r}_i$ in Λ.

For later use we introduce the set of grid points with non-zero frequencies

$$\Gamma^{(n),N}_{\Lambda,\alpha} := \left\{ \frac{\boldsymbol{\ell}}{N} \middle| \boldsymbol{\ell} \in (\mathbb{Z}/N\mathbb{Z})^2, \nu^{(n),N}_{\Lambda,\alpha}(\boldsymbol{\ell}) \neq 0 \right\}. \tag{60}$$

5.1.1. Hyperbolic regime with D randomly chosen points $\boldsymbol{r}_i$ in Λ. In the hyperbolic regime corresponding to $\alpha \in \mathbb{Z} \setminus \{-4, -3, -2, -1, \quad 0\}$, $\Gamma^{(n),N}_{\Lambda,\alpha}$ tends to increase its cardinality with the number of timesteps n. Roughly speaking, there appear to be two distinct temporal patterns: a first one, during which $\#\left(\Gamma^{(n),N}_{\Lambda,\alpha}\right) \simeq D^n \leqslant N^2$ and almost every $\nu^{(n),N}_{\Lambda,\alpha} \simeq D^{-n}$, followed by a second one characterized by frequencies frozen to $\nu^{(n),N}_{\Lambda,\alpha}(\boldsymbol{\ell}) = \frac{1}{N^2}, \forall \boldsymbol{\ell} \in (\mathbb{Z}/N\mathbb{Z})^2$. The second temporal pattern is reached when, during the first one, $\Gamma^{(n),N}_{\Lambda,\alpha}$ has covered the whole lattice and $D^n \simeq N^2$.

From the point of view of the entropies, the first temporal regime is characterized by

$$H_{\omega_{N^2}}(\alpha, \Lambda, n) \sim n \cdot \log D \qquad h_{\omega_{N^2},\mathcal{W}_\infty}(\alpha, \Lambda, n) \sim \log D$$

while the second one by

$$H_{\omega_{N^2}}(\alpha, \Lambda, n) \sim 2 \log N \qquad h_{\omega_{N^2},\mathcal{W}_\infty}(\alpha, \Lambda, n) \sim \frac{2 \log N}{n}.$$

The transition between these two regimes occurs at $\bar{n} = \log_D N^2$. However, this time cannot be considered a realistic breaking-time, as it too strongly depends on the chosen partition.

Figure 2 (columns (a and (c)) shows the mechanism clearly in a density plot: white or light-grey points correspond to points of $\Gamma^{(n),N}_{\Lambda,\alpha}$ and their number increases for small numbers of iterations until the plot assumes a uniform grey colour for large n.

The linear and stationary behaviour of $H_{\omega_{N^2}}(\alpha, \Lambda, n)$ is apparent in figure 4, where four different plateaus ($2 \log N$) are reached for four different N, and in figure 5, in which four different slopes are shown for four different numbers of elements in the partition. With the same parameters as in figure 5, figure 6 shows the corresponding entropy production $h_{\omega_{N^2},\mathcal{W}_\infty}(\alpha, \Lambda, n)$.

5.1.2. Hyperbolic regime with D nearest neighbours $\boldsymbol{r}_i$ in Λ. In the following, we will consider a set of points $\Lambda = \{\boldsymbol{r}_i\}_{i=1\ldots D}$ very close to each other, instances of which are shown in figure 1.

From equations (54) and (55), the frequencies $\nu^{(n),N}_{\Lambda,\alpha}(\boldsymbol{\ell})$ result proportional to how many strings have equal images $\boldsymbol{\ell}$, through the function $\boldsymbol{f}^{(n),N}_{\Lambda,\alpha}$ in (53). Due to the fact that $[T_\alpha]_{11} = [T_\alpha]_{21} = 1$, non-injectivity of $\boldsymbol{f}^{(n),N}_{\Lambda,\alpha}$ occurs very frequently when $\{\boldsymbol{r}_i\}$ are very close to each other. This is a dynamical effect that, in continuous systems [14], leads to an entropy production approaching the Lyapounov exponent. Even in the discrete case, during a finite time interval though, $h_{\omega_{N^2},\mathcal{W}_\infty}(\alpha, \Lambda, n)$ exhibits the same behaviour until $H_{\omega_{N^2}}$ reaches the upper bound $2 \log N$. From then on, the system behaves as described in section 5.1.1, and the entropy production goes to zero as

$$h_{\omega_{N^2},\mathcal{W}_\infty}(\alpha, \Lambda, n) \sim \frac{1}{n} \quad \text{(see figure 7)}.$$

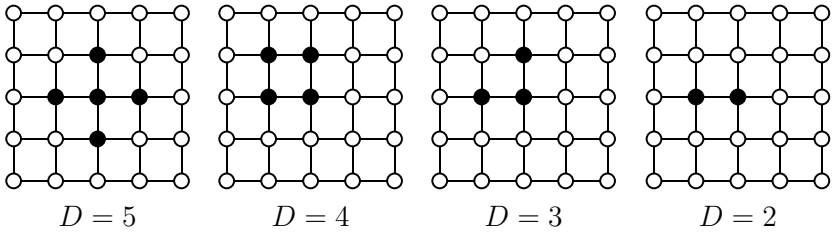

Figure 1. Several combinations of D nearest neighbours in Λ for different values D.

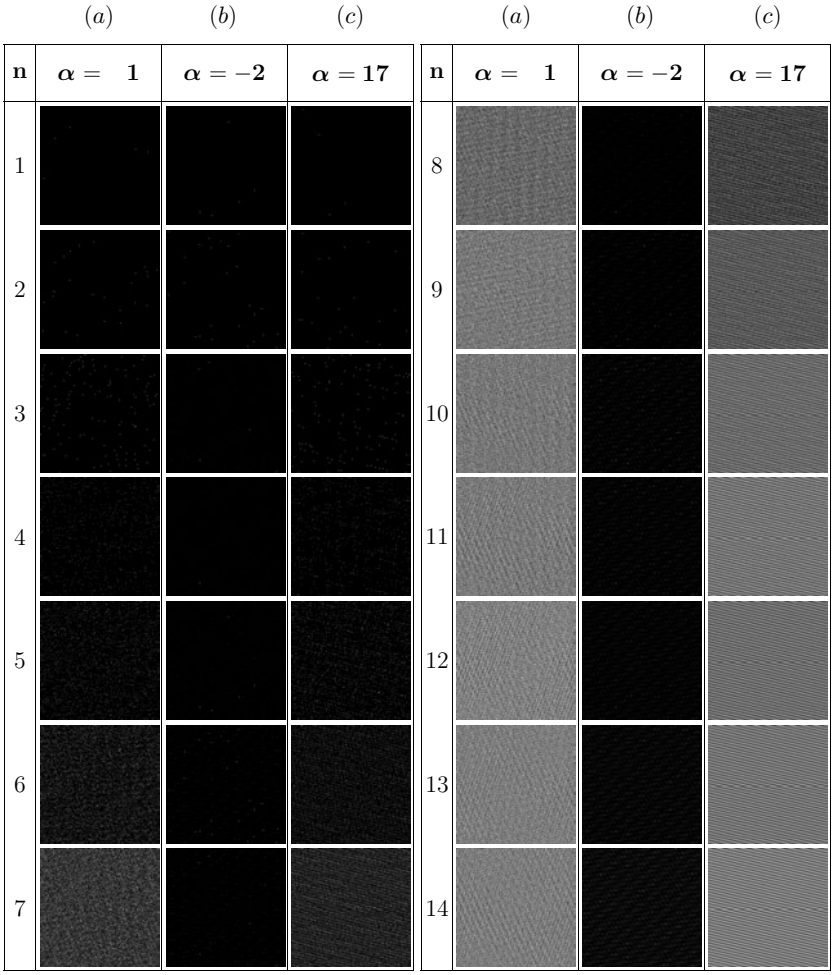

Figure 2. Density plots showing the frequencies $\nu_{\Lambda,\alpha}^{(n),N}$ in two hyperbolic regimes (columns (a) and (c)) and an elliptic one (column (b)), for five randomly distributed $\boldsymbol{r}_i$ in Λ with $N = 200$. Black corresponds to $\nu_{\Lambda,\alpha}^{(n),N} = 0$. In the hyperbolic cases, $\nu_{\Lambda,\alpha}^{(n),N}$ tends to equidistribute on $(\mathbb{Z}/N\mathbb{Z})^2$ with increasing n and becomes constant when the breaking-time is reached.

Concerning figure 3 (column (d)), whose corresponding graph for $h_{\omega_{N^2},\mathcal{W}_\infty}(1, \Lambda, n)$ is labelled by $\triangleright$ in figure 7, we make the following consideration:

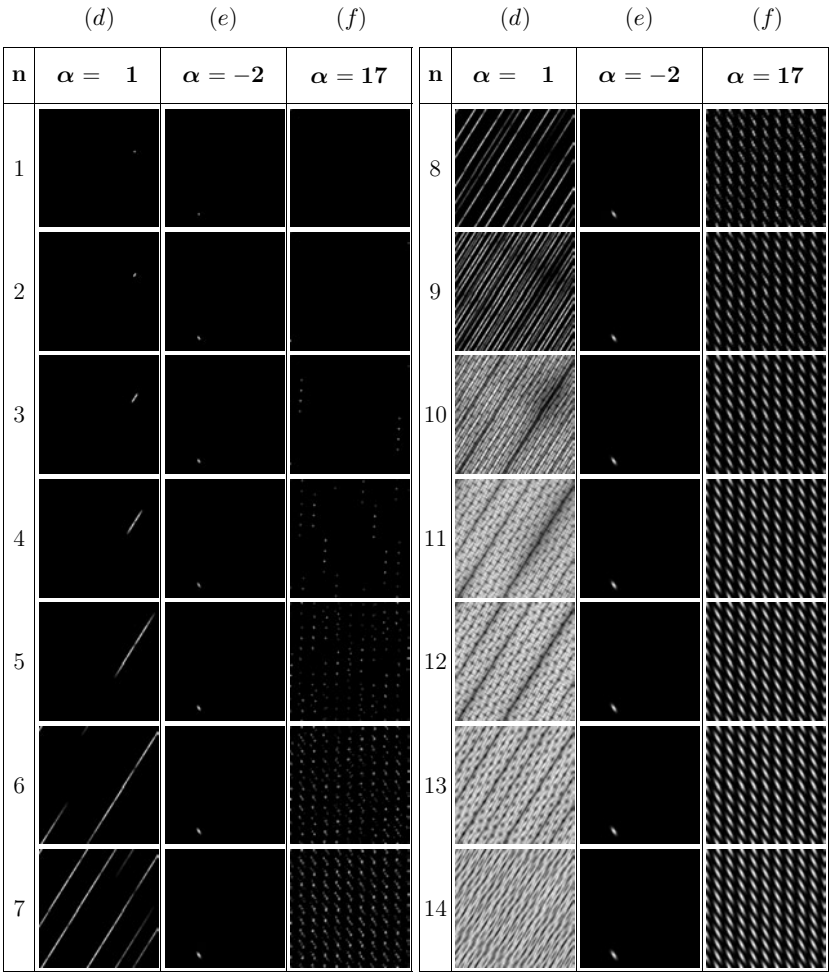

Figure 3. Density plots showing $\nu^{(n),N}_{\Lambda,\alpha}$ in two hyperbolic (columns (d) and (f)) and one elliptic (column (e)) regime, for five nearest neighbouring $\boldsymbol{r}_i$ in Λ ($N = 200$). Black corresponds to $\nu^{(n),N}_{\Lambda,\alpha} = 0$. When the system is chaotic, the frequencies tend to equidistribute on $(\mathbb{Z}/N\mathbb{Z})^2$ with increasing n and to approach, when the breaking-time is reached, the constant value $\frac{1}{N^2}$. Column (f) shows how the dynamics can be confined on a sublattice by a particular combination (α, N, Λ) with a corresponding entropy decrease.

- for $n = 1$ the white spot corresponds to five $\boldsymbol{r}_i$ grouped as in figure 1. In this case $h_{\omega_{N^2},\mathcal{W}_\infty}(1, \Lambda, 1) = \log D = \log 5$;
- for $n \in [2, 5]$ the white spot begins to stretch along the stretching direction of T_1. In this case, the frequencies $\nu^{(n),N}_{\Lambda,\alpha}$ are not constant on the light-grey region: this leads to a decrease of $h_{\omega_{N^2},\mathcal{W}_\infty}(1, \Lambda, n)$;
- for $n \in [6, 10]$ the light-grey region becomes so elongated that it starts feeling the folding condition so that, with increasing timesteps, it eventually fully covers the originally dark space. In this case, the behaviour of $h_{\omega_{N^2},\mathcal{W}_\infty}(1, \Lambda, n)$ remains the same as before up to $n = 10$;
- for $n = 11$, $\Gamma^{(n),N}_{\Lambda,\alpha}$ coincides with the whole lattice;

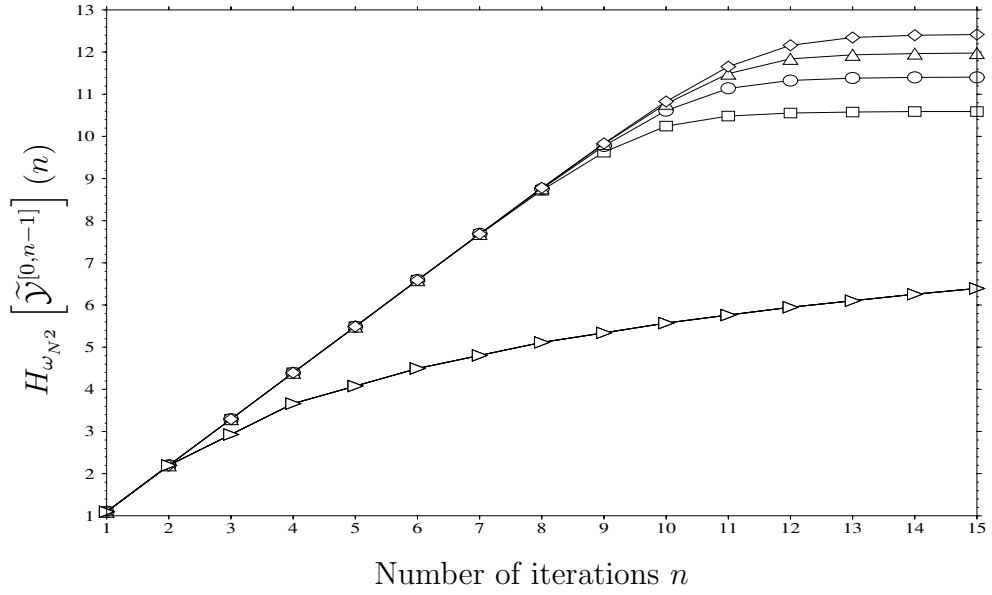

Figure 4. Von Neumann entropy $H_{\omega_{N^2}}(n)$ in four hyperbolic ($\alpha = 1$ for $\diamondsuit$, $\triangle$, $\bigcirc$, $\square$) and four elliptic ($\alpha = -2$ for $\triangleright$) cases, for three randomly distributed $\boldsymbol{r}_i$ in Λ. Values for N are: $\diamondsuit = 500$, $\triangle = 400$, $\bigcirc = 300$ and $\square = 200$, whereas the curve labelled by $\triangleright$ represents four elliptic systems with $N \in \{200, 300, 400, 500\}$.

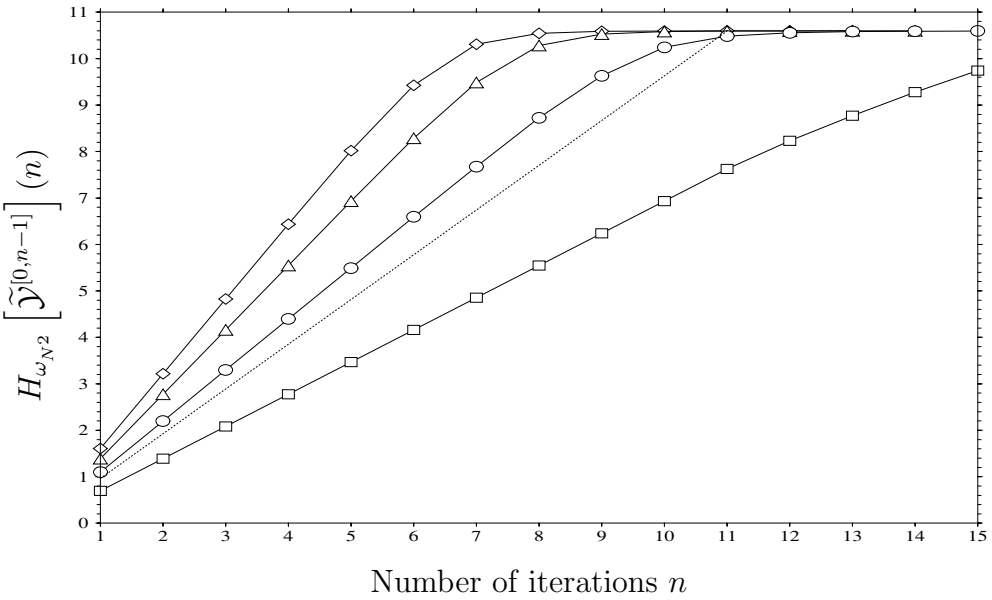

Figure 5. Von Neumann entropy $H_{\omega_{N^2}}(n)$ in four hyperbolic ($\alpha = 1$) cases, for D randomly distributed $\boldsymbol{r}_i$ in Λ, with $N = 200$. Value for D are: $\diamondsuit = 5$, $\triangle = 4$, $\bigcirc = 3$ and $\square = 2$. The dotted line represents $H_{\omega_{N^2}}(n) = \log\lambda \cdot n$, where $\log\lambda = 0.962\ldots$ is the Lyapounov exponent at $\alpha = 1$.

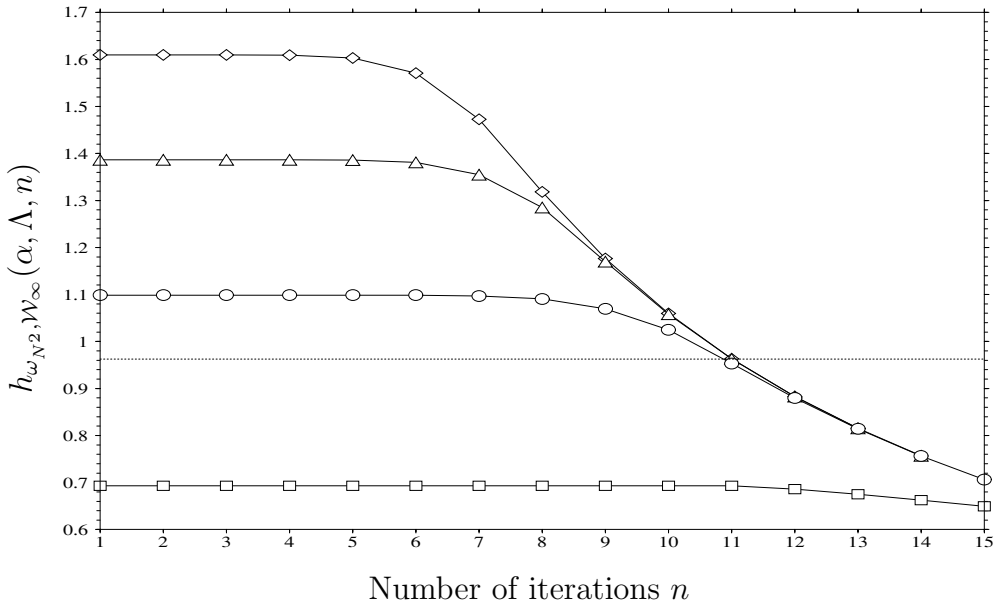

Figure 6. Entropy production $h_{\omega_{N^2},\mathcal{W}_\infty}(\alpha, \Lambda, n)$ in four hyperbolic ($\alpha = 1$) cases, for D randomly distributed $\boldsymbol{r}_i$ in Λ, with $N = 200$. Values for D are: $\Diamond = 5$, $\triangle = 4$, $\bigcirc = 3$ and $\square = 2$. The dotted line corresponds to the Lyapounov exponent $\log\lambda = 0.962\ldots$ at $\alpha = 1$.

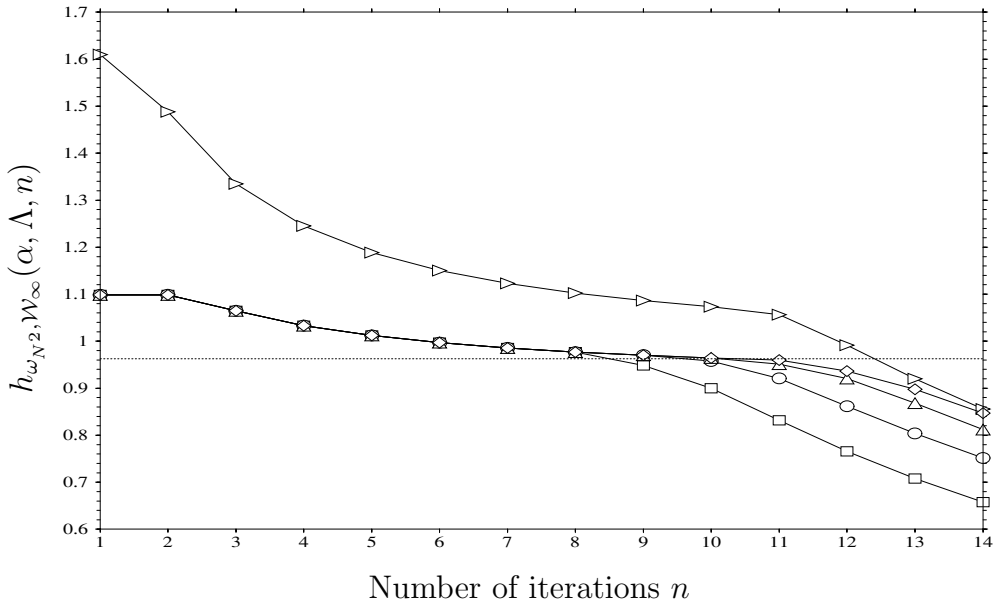

Figure 7. Entropy production $h_{\omega_{N^2},\mathcal{W}_\infty}(\alpha, \Lambda, n)$ in five hyperbolic ($\alpha = 1$) cases, for D nearest neighbouring points $\boldsymbol{r}_i$ in Λ. Values for (N, D) are: $\triangleright = (200, 5)$, $\Diamond = (500, 3)$, $\triangle = (400, 3)$, $\bigcirc = (300, 3)$ and $\square = (200, 3)$. The dotted line corresponds to the Lyapounov exponent $\log\lambda = 0.962\ldots$ at $\alpha = 1$ and represents the natural asymptote for all these curves in the absence of breaking-time.

- for larger times, the frequencies $\nu_{\Lambda,1}^{(n),N}$ tend to the constant value $\frac{1}{N^2}$ at almost every point of the grid. In this case, the behaviour of the entropy production undergoes a critical change (the crossover occurring at $n = 11$) as shown in figure 7.

Again, we cannot conclude that $n = 11$ is a realistic breaking-time, because once more we have strong dependence on the chosen partition (namely from the number D of its elements). For instance, in figure 7, one can see that partitions with three points reach their corresponding 'breaking-times' faster than that with $D = 5$; also they do it in an N-dependent way.

For a chosen set Λ consisting of D elements very close to each other and N very large, $h_{\omega_{N^2},\mathcal{W}_\infty}(\alpha, \Lambda, n) \simeq \log\lambda$ (which is the asymptote in the continuous case) from a certain $\bar{n}$ up to a time τ_B. Since this latter is now partition independent, it can properly be considered as the breaking-time of the system; it is given by

$$\tau_B = \log_\lambda N^2. \tag{61}$$

It is evident from equation (61) that if one knows τ_B then also $\log\lambda$ is known. Usually, one is interested in the latter which is a sign of the instability of the continuous classical system. In the following, we develop an algorithm which allows us to extract $\log\lambda$ from studying the corresponding discretized classical system and its ALF-entropy.

In working conditions, N is not large enough to allow for $\bar{n}$ being smaller than τ_B; what happens in such a case is that $H_{\omega_{N^2}}(\alpha, \Lambda, n) \simeq 2\log N$ before the asymptote for $h_{\omega_{N^2},\mathcal{W}_\infty}(\alpha, \Lambda, n)$ is reached. Given $h_{\omega_{N^2},\mathcal{W}_\infty}(\alpha, \Lambda, n)$ for $n < \tau_B$, it is thus necessary to seek means how to estimate the long time behaviour that one would have if the system were continuous.

Remark 5.1. When estimating Lyapounov exponents from discretized hyperbolic classical systems, by using partitions consisting of the nearest neighbours, we have to take into account some facts:

(a) $h_{\omega_{N^2},\mathcal{W}_\infty}(\alpha, \Lambda, n)$ does not increase with n; therefore, if $D < \lambda$, $h_{\omega_{N^2},\mathcal{W}_\infty}$ cannot reach the Lyapounov exponent. Denoted by $\log\lambda(D)$ the asymptote that we extrapolate from the data[4], in general we have $\lambda(D) \leqslant \log D < \lambda$. For instance, for $\alpha = 1$, $\lambda = 2.618\ldots > 2$ and partitions with $D = 2$ cannot produce an entropy greater than $\log 2$; this is the case for the entropies below the dotted line in figures 5 and 6;

(b) partitions with D small but greater than λ allow $\log\lambda$ to be reached in a very short time and $\lambda(D)$ is very close to λ in this case;

(c) partitions with $D \gg \lambda$ require a very long time to converge to $\log\lambda$ (and so very large N) and, moreover, it is not a trivial task to deal with them from a computational point of view. In contrast, the entropy behaviour for such partitions offers very good estimates of λ (compare, in figure 7, $\triangleright$ with $\Diamond$, $\triangle$, $\circ$ and $\square$);

(d) in order to compute λ (and then τ_B, by (61)), one can calculate $\lambda(D)$ for increasing D, until it converges to a stable value λ;

(e) due to a number of theoretical reasons, the UMG on $(\mathbb{Z}/N\mathbb{Z})^2$ present several anomalies. An instance of them is shown in figure 3 (column (f)), where a partition with five nearest neighbours on a lattice of 200×200 points confines the image of $\boldsymbol{f}_{\Lambda,\alpha}^{(n),N}$ (under the action of a T_α map with $\alpha = 17$) on a subgrid of the torus. In this and analogous cases, there occurs an anomalous depletion of the entropy production and no significant information is obtainable from it. To avoid these difficulties, in section 5.2 we will go beyond the UMG subclass considered so far.

[4] $h_{\omega_{N^2},\mathcal{W}_\infty}(\alpha, \Lambda, n)$ may even equal $\log\lambda(D)$ from the start.

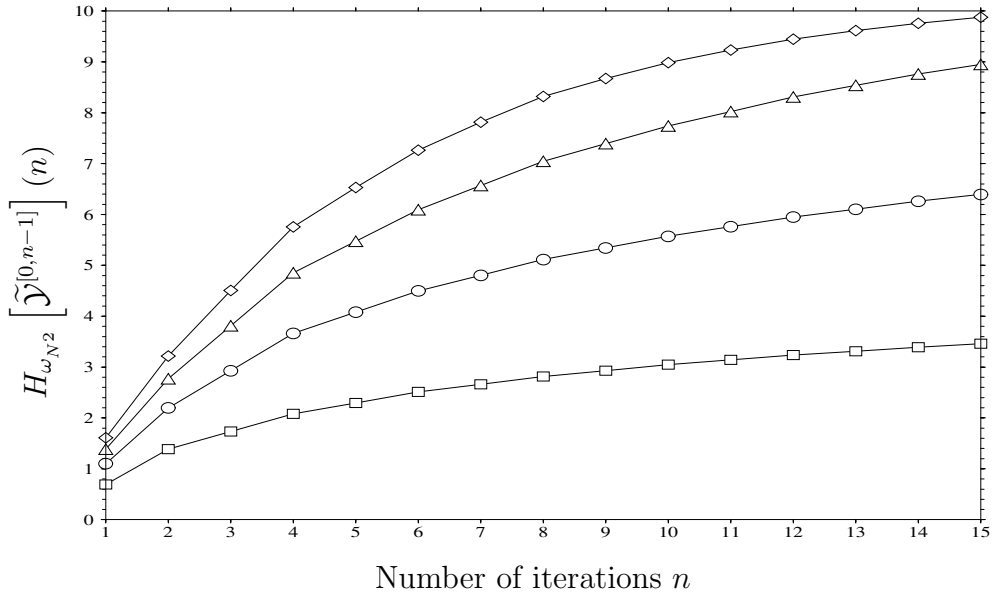

Figure 8. Von Neumann entropy $H_{\omega_{N^2}}(n)$ in four elliptic ($\alpha = -2$) cases, for D randomly distributed $\boldsymbol{r}_i$ in Λ, with $N = 200$. Values for D are: $\diamondsuit = 5$, $\triangle = 4$, $\bigcirc = 3$ and $\square = 2$.

5.1.3. Elliptic regime ($\alpha \in \{-1, -2, -3\}$). One can show that all evolution matrices T_α are characterized by the following property:

$$T_\alpha^2 = \bar{\alpha} T_\alpha - \mathbb{1} \qquad \bar{\alpha} := (\alpha + 2). \tag{62}$$

In the elliptic regime $\alpha \in \{-1, -2, -3\}$, therefore $\bar{\alpha} \in \{-1, 0, 1\}$ and relation (62) determines a periodic evolution with periods:

$$T_{-1}^3 = -\mathbb{1} \qquad \left(T_{-1}^6 = \mathbb{1}\right) \tag{63a}$$

$$T_{-2}^2 = -\mathbb{1} \qquad \left(T_{-2}^4 = \mathbb{1}\right) \tag{63b}$$

$$T_{-3}^3 = +\mathbb{1}. \tag{63c}$$

It has to be stressed that, in the elliptic regime, the relations (63) do not hold 'modulo N', instead they are completely independent of N.

Due to the high degree of symmetry in relations (62), (63), the frequencies $\nu_{\Lambda,\alpha}^{(n),N}$ are different from zero only on a small subset of the whole lattice.

This behaviour is apparent in figure 2 column (b), in which we consider five randomly distributed $\boldsymbol{r}_i$ in Λ, and in figure 3 column (e), in which the five $\boldsymbol{r}_i$ are grouped as in figure 1. In both cases, the von Neumann entropy $H_{\omega_{N^2}}(n)$ is not linearly increasing with n (see figure 8), instead it assumes a log-shaped profile (up to the breaking-time, see figure 4).

Remark 5.2. The last observation indicates how the entropy production analysis can be used to recognize whether a dynamical system is hyperbolic or not. If we use randomly distributed points as a partition, we observe that hyperbolic systems show constant entropy production (up to the breaking-time), whereas the others do not.

Moreover, unlike hyperbolic ones, elliptic systems do not change their behaviour with N (for reasonably large N) as clearly shown in figure 4, in which elliptic systems ($\alpha = -2$) with

four different values of N give the same plot. In contrast, we have a dependence on how rich is the chosen partition, similarly to what we have for hyperbolic systems, as shown in figure 7.

5.1.4. Parabolic regime ($\alpha \in \{0, 4\}$). This regime is characterized by $\lambda = \lambda^{-1} = \pm 1$, that is $\log|\lambda| = 0$ (see remark 2.1 (c)). These systems behave as hyperbolic ones (see sections 5.1.1 and 5.1.2) and this is also true for the general behaviour of the entropy production, apart from the fact that we never fall in condition (a) of remark 5.1. Then, for sufficiently large N, every partition consisting of D grouped $\boldsymbol{r}_i$ will reach the asymptote $\log|\lambda| = 0$.

5.2. The case of sawtooth maps

The sawtooth maps [15, 16] are triples $(\mathcal{X}, \mu, S_\alpha)$ where

$$\mathcal{X} = \mathbb{T}^2 = \mathbb{R}^2/\mathbb{Z}^2 = \{\boldsymbol{x} = (x_1, x_2) \pmod 1\} \tag{64a}$$

$$S_\alpha \begin{pmatrix} x_1 \\ x_2 \end{pmatrix} = \begin{pmatrix} 1+\alpha & 1 \\ \alpha & 1 \end{pmatrix} \begin{pmatrix} \langle x_1 \rangle \\ x_2 \end{pmatrix} \pmod 1 \qquad \alpha \in \mathbb{R} \tag{64b}$$

$$\mathrm{d}\mu(\boldsymbol{x}) = \mathrm{d}x_1\,\mathrm{d}x_2 \tag{64c}$$

where $\langle\cdot\rangle$ denotes the fractional part of a real number. Without $\langle\cdot\rangle$, (64*b*) is not well defined on $\mathbb{T}^2$ for non-integer α; in fact, without taking the fractional part, the same point $\boldsymbol{x} = \boldsymbol{x} + \boldsymbol{n} \in \mathbb{T}^2$, $\boldsymbol{n} \in \mathbb{Z}^2$, would have (in general) $S_\alpha(\boldsymbol{x}) \neq S_\alpha(\boldsymbol{x} + \boldsymbol{n})$. Of course, $\langle\cdot\rangle$ is not necessary when $\alpha \in \mathbb{Z}$.

The Lebesgue measure defined in (64*c*) is *invariant* for all $\alpha \in \mathbb{R}$. After identifying $\boldsymbol{x}$ with canonical coordinates (q, p) and imposing the (mod 1) condition on both of them, the above dynamics can be rewritten as

$$\begin{cases} q' = q + p' \\ p' = p + \alpha\langle q \rangle \end{cases} \pmod 1. \tag{65}$$

This is nothing but the Chirikov standard map [4] in which $-\frac{1}{2\pi}\sin(2\pi q)$ is replaced by $\langle q \rangle$. The dynamics in (65) can also be thought of as generated by the (singular) Hamiltonian

$$H(q, p, t) = \frac{p^2}{2} - \alpha\frac{\langle q \rangle^2}{2}\delta_p(t) \tag{66}$$

where $\delta_p(t)$ is the periodic Dirac delta which makes the potential act through periodic kicks with period 1.

Sawtooth maps are invertible and the inverse is given by the expression

$$S_\alpha^{-1} \begin{pmatrix} x_1 \\ x_2 \end{pmatrix} = \begin{pmatrix} 1 & 0 \\ -\alpha & 1 \end{pmatrix} \left\langle \begin{pmatrix} 1 & -1 \\ 0 & 1 \end{pmatrix} \begin{pmatrix} x_1 \\ x_2 \end{pmatrix} \right\rangle \pmod 1 \tag{67}$$

or, in other words,

$$\begin{cases} q = q' - p' \\ p = -\alpha q + p' \end{cases} \pmod 1. \tag{68}$$

It can indeed be checked that $S_\alpha\big(S_\alpha^{-1}(\boldsymbol{x})\big) = S_\alpha^{-1}(S_\alpha(\boldsymbol{x})) = \langle \boldsymbol{x} \rangle$, $\forall \boldsymbol{x} \in \mathbb{T}^2$.

Remark 5.3.

(i) Sawtooth maps $\{S_\alpha\}$ are *discontinuous* on the subset $\gamma_0 := \{\boldsymbol{x} = (0, p),\ p \in \mathbb{T}\} \in \mathbb{T}^2$: two points close to this border, $A := (\varepsilon, p)$ and $B := (1 - \varepsilon, p)$, have images that differ, in the $\varepsilon \to 0$ limit, by a vector $d^{(1)}_{S_\alpha}(A, B) = (\alpha, \alpha) \pmod 1$.

(ii) Inverse sawtooth maps $\{S_\alpha^{-1}\}$ are *discontinuous* on the subset $\gamma_{-1} := S_\alpha(\gamma_0) = \{x = (p, p), p \in \mathbb{T}\} \in \mathbb{T}^2$: two points close to this border, $A := (p + \varepsilon, p - \varepsilon)$ and $B := (p - \varepsilon, p + \varepsilon)$, have images that differ, in the $\varepsilon \to 0$ limit, by a vector $d^{(1)}_{S_\alpha^{-1}}(A, B) = (0, \alpha) \pmod 1$.

(iii) The hyperbolic, elliptic or parabolic behaviour of sawtooth maps is related to the eigenvalues of $\left(\begin{smallmatrix} 1+\alpha & 1 \\ \alpha & 1 \end{smallmatrix}\right)$ exactly as in remark 2.1 (ii).

(iv) The Lebesgue measure in (64*c*) is S_α^{-1}-invariant.

From a computational point of view, the study of the entropy production in the case of sawtooth maps S_α is more complicated than for the T_α. The reason to study these dynamical systems numerically is twofold:

- to avoid the difficulties described in remark 5.1 (e);
- to deal, in a way compatible with numerical computation limits, with the largest possible spectrum of accessible Lyapounov exponent. We know that for $\alpha \in \mathbb{Z} \bigcap \{\text{non-elliptic domain}\}$,

$$\lambda^{\pm}(T_\alpha) = \lambda^{\pm}(S_\alpha) = \frac{\alpha + 2 \pm \sqrt{(\alpha+2)^2 - 4}}{2}.$$

  In order to fit $\log \lambda_\alpha$ ($\log \lambda_\alpha$ being the Lyapounov exponent corresponding to a given α) via entropy production analysis, we need D elements in the partition (see points (b) and (c) of remark 5.1) with $D \geqslant \lambda_\alpha$. Moreover, if we were to study the power of our method for different integer values of α we would be forced to use very large D, in which case we would need very long computing times in order to evaluate numerically the entropy production $h_{\omega_{N^2}, \mathcal{W}_\infty}(\alpha, \Lambda, n)$ in a reasonable interval of times n. Instead, for sawtooth maps, we can fix the parameters (N, D, Λ) and study λ_α for α confined in a small domain, but free to assume every real value in that domain.

In the following, we investigate the case of α in the hyperbolic regime with D nearest neighbours $\boldsymbol{r}_i$ in Λ, as done in section 5.1.2. In particular, figures 9–12 refer to the following fixed parameters:

$N = 38 \qquad n_{\max} = 5 \qquad D = 5$

$$\Lambda: \qquad \boldsymbol{r}_1 = \begin{pmatrix} 7 \\ 8 \end{pmatrix} \qquad \boldsymbol{r}_2 = \begin{pmatrix} 7 \\ 9 \end{pmatrix} \qquad \boldsymbol{r}_3 = \begin{pmatrix} 6 \\ 8 \end{pmatrix} \qquad \boldsymbol{r}_4 = \begin{pmatrix} 7 \\ 7 \end{pmatrix} \qquad \boldsymbol{r}_5 = \begin{pmatrix} 8 \\ 8 \end{pmatrix};$$

α : from 0.00 to 1.00 with an incremental step of 0.05.

First, we compute the von Neumann entropy (49) using the (Hermitian) matrix $\mathcal{G}_{\ell_1,\ell_2}(n)$ defined in (48). This is actually a diagonalization problem: once the N^2 eigenvalues $\{\eta_i\}_{i=1}^{N^2}$ are found, then

$$H_{\omega_{N^2}}[\tilde{\mathcal{Y}}^{[0,n-1]}] = -\sum_{i=1}^{N^2} \eta_i \log \eta_i. \tag{69}$$

Then, from (59), we can determine $h_{\omega_{N^2}, \mathcal{W}_\infty}(\alpha, \Lambda, n)$. In the numerical example, the (Λ-dependent) breaking-time occurs after $n = 5$; for this reason we have chosen $n_{\max} = 5$. In fact, we are interested in the region where the discrete system behaves almost as a continuous one.

In figure 9, the entropy production is plotted for the chosen set of α: for very large N (that is close to the continuum limit, in which no breaking-time occurs) all curves (characterized by different α) would tend to $\log \lambda_\alpha$ with n.

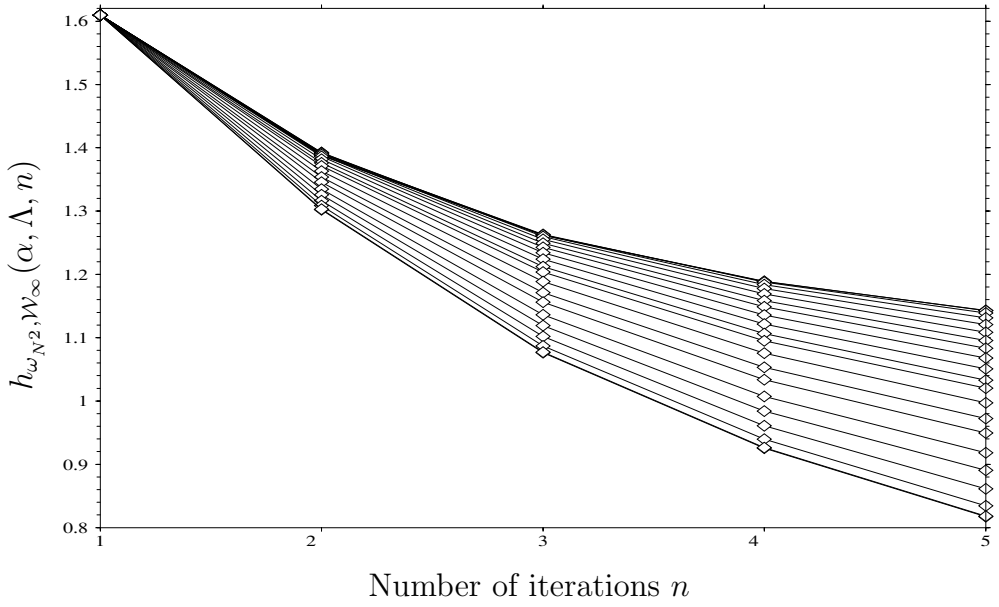

Figure 9. Entropy production $h_{\omega_{N^2},\mathcal{W}_\infty}(\alpha, \Lambda, n)$ for 21 hyperbolic sawtooth maps, relative to a for a cluster of five nearest neighbourings points $\boldsymbol{r}_i$ in Λ, with $N = 38$. The parameter α decreases from $\alpha = 1.00$ (corresponding to the upper curve) to $\alpha = 0.00$ (lower curve) through 21 equispaced steps.

One way to determine the asymptote $\log \lambda_\alpha$ is to fit the decreasing function $h_{\omega_{N^2},\mathcal{W}_\infty}(\alpha, \Lambda, n)$ over the range of data and extrapolate the fit for $n \to \infty$. Of course, we cannot perform the fit with polynomials, because every polynomial diverges in the $n \to \infty$ limit.

A better strategy is to compactify the time evolution by means of a isomorphic positive function s with bounded range, for instance,

$$\mathbb{N} \ni n \longmapsto s_n := \frac{2}{\pi} \arctan(n-1) \in [0, 1]. \tag{70}$$

Then, for fixed α, in figure 10 we consider $n_{\max}$ points $\left(s_n, h_{\omega_{N^2},\mathcal{W}_\infty}(\alpha, \Lambda, n)\right)$ and extract the asymptotic value of $h_{\omega_{N^2},\mathcal{W}_\infty}(\alpha, \Lambda, n)$ for $n \to \infty$, that is the value of $h_{\omega_{N^2},\mathcal{W}_\infty}(\alpha, \Lambda, s^{-1}(t))$ for $t \to 1^-$, as follows.

Given a graph consisting of $m \in \{2, 3, \ldots, n_{\max}\}$ points, in our case the first m points of curves as in figure 10, namely

$$\left\{\left(s_1, h_{\omega_{N^2},\mathcal{W}_\infty}(\alpha, \Lambda, 1)\right), \left(s_2, h_{\omega_{N^2},\mathcal{W}_\infty}(\alpha, \Lambda, 2)\right), \ldots, \left(s_m, h_{\omega_{N^2},\mathcal{W}_\infty}(\alpha, \Lambda, m)\right)\right\}$$

the data are fit by a Lagrange polynomial $\mathcal{P}^m(t)$ (of degree $m-1$)

$$\mathcal{P}^m(t) = \sum_{i=1}^{m} P_i(t) \tag{71a}$$

where

$$P_i(t) = \prod_{\substack{j=1 \\ j \neq i}}^{m} \frac{t - s_j}{s_i - s_j} h_{\omega_{N^2},\mathcal{W}_\infty}(\alpha, \Lambda, i). \tag{71b}$$

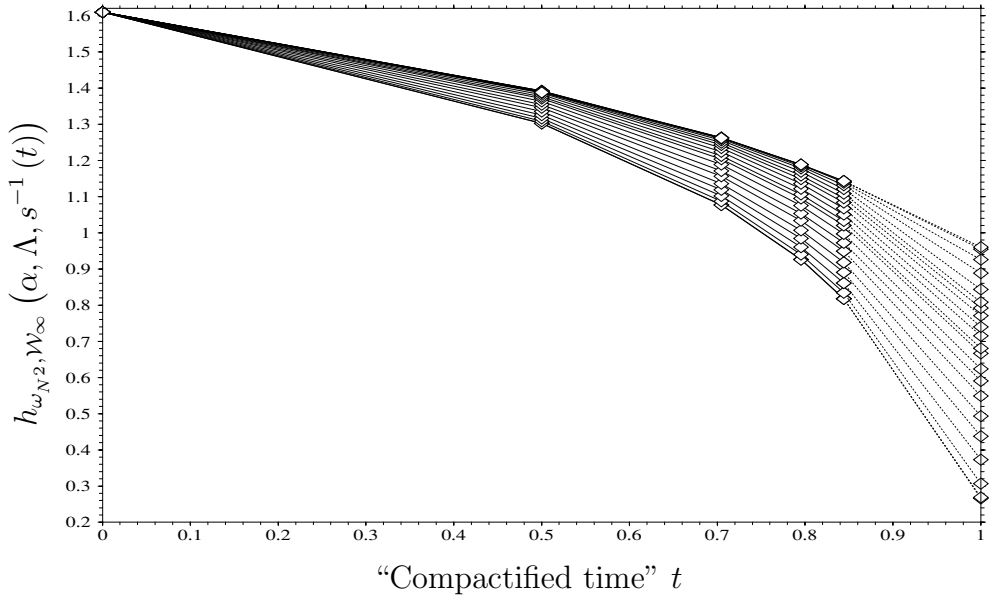

Figure 10. The solid lines correspond to $(s_n, h_{\omega_{N^2},\mathcal{W}_\infty}(\alpha,\Lambda,n))$, with $n \in \{1,2,3,4,5\}$, for the values of α considered in figure 9. Every α-curve is continued as a dotted line up to $(1, l_\alpha^5)$, where l_α^5 is the Lyapounov exponent extracted from the curve by fitting all five points via a Lagrange polynomial $\mathcal{P}^m(t)$.

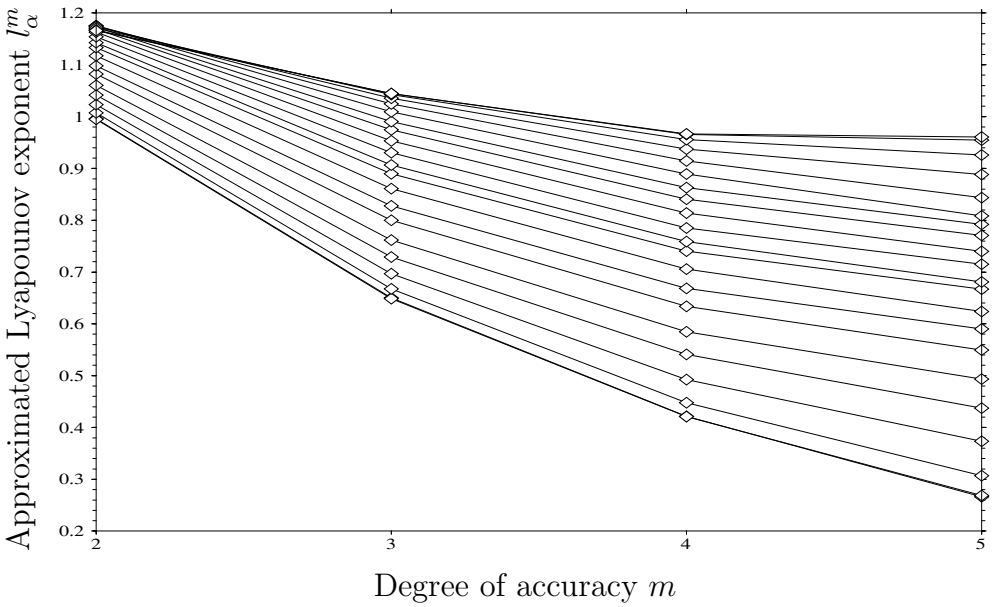

Figure 11. Four estimated Lyapounov exponents l_α^m plotted versus their degree of accuracy m for the values of α considered in figures 9 and 10.

The value assumed by this polynomial when $t \to 1^-$ (corresponding to $n \to \infty$) will be the estimate (of degree m) of the Lyapounov exponent, denoted by l_α^m: the higher the value of m,

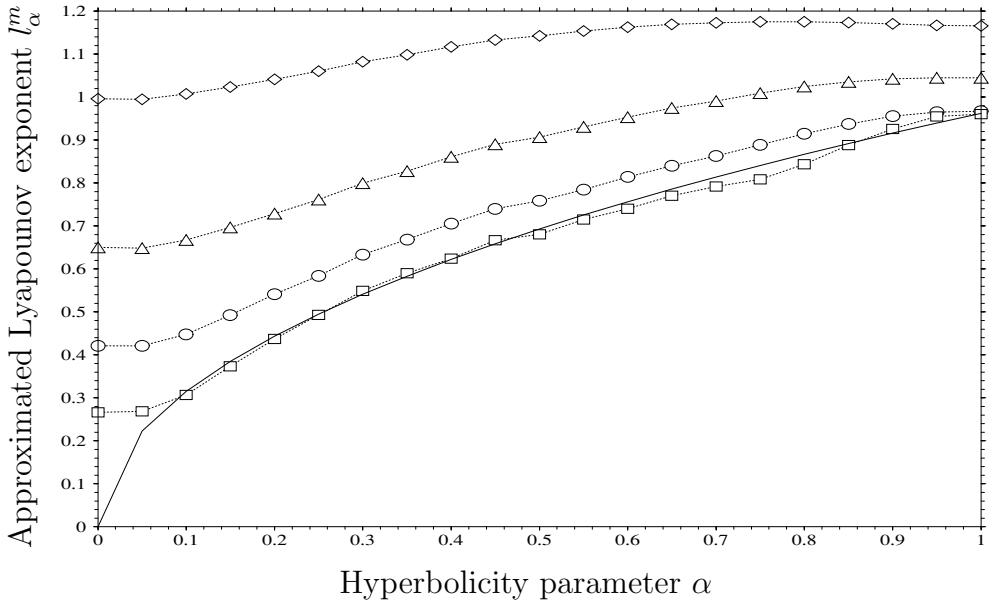

Figure 12. Plots of the four estimated Lyapounov exponents l_α^m of figure 11 versus the considered values of α. The polynomial degree m is as follows: $\Diamond = 2$, $\triangle = 3$, $\circ = 4$ and $\square = 5$. The solid line corresponds to the theoretical Lyapounov exponent $\log \lambda_\alpha = \log(\alpha + 2 + \sqrt{\alpha\,(\alpha+4)}) - \log 2$.

the more accurate the estimate. From (71) we get

$$l_\alpha^m := \mathcal{P}^m(t)|_{t=1} = \sum_{i=1}^{m} h_{\omega_{N^2},\mathcal{W}_\infty}(\alpha, \Lambda, i) \prod_{\substack{j=1 \\ j\neq i}}^{m} \frac{1 - s_j}{s_i - s_j}. \tag{72}$$

The various l_α^m are plotted in figure 11 as functions of m for all considered α. The convergence of l_α^m with m is shown in figure 12, together with the theoretical Lyapounov exponent $\log \lambda_\alpha$; as expected, we find that the latter is the asymptote of $\{l_\alpha^m\}_m$ with respect to the polynomial degree m.

The dotted line in figure 10 extrapolates 21 α-curves in compactified time up to $t = 1$ using five points in the Lagrange polynomial approximation.

6. Conclusions

In this paper, we have considered discretized hyperbolic classical systems on the torus by forcing them on a squared lattice with spacing $\frac{1}{N}$. We showed how the discretization procedure is similar to quantization; in particular, following the analogous case of the classical limit $\hbar \longmapsto 0$, we have set up the theoretical framework to discuss the continuous limit $N \longmapsto \infty$. Furthermore, using the similarities between discretized and quantized classical systems, we have applied the quantum dynamical entropy of Alicki and Fannes to study the footprints of classical (continuous) chaos as it is expected to reveal itself, namely through the presence of characteristic time scales and corresponding breaking-times. Indeed, exactly as in quantum chaos, a discretized hyperbolic system can mimic its continuous partner only up to times which scale as $\log N$. We have also extended the numerical analysis from the so-called Arnold cat

maps to the discontinuous sawtooth maps, whose interpretation in the theoretical frame set up in this work will be discussed in a forthcoming paper.

Acknowledgment

This work is supported in part by CONACyT project number U40004-F.

References

[1] Devaney R 1989 *An Introduction to Chaotic Dynamical Systems* (Reading, MA: Addison-Wesley)
[2] Wiggins S 1990 *Dynamical Systems and Chaos* (New York: Springer)
[3] Katok A and Hasselblatt B 1999 *Introduction to the Modern Theory of Dynamical Systems* (Cambridge: Cambridge University Press)
[4] Casati G and Chirikov B 1995 *Quantum Chaos. Between Order and Disorder* (Cambridge: Cambridge University Press)
[5] Crisanti A, Falcioni M and Vulpiani A 1993 Transition from regular to complex behavior in a discrete deterministic asymmetric neural network model *J. Phys. A: Math. Gen.* **26** 3441
[6] Crisanti A, Falcioni M, Mantica G and Vulpiani A 1994 Applying algorithmic complexity to define chaos in the motion of complex systems *Phys. Rev.* E **50** 1959–67
[7] Boffetta G, Cencini M, Falcioni M and Vulpiani A 2001 Predictability: a way to characterize 'Complexity' *Preprint* nlin. CD/0101029
[8] Zertuche F, López-Peña R and Waelbroeck H 1994 Recognition of temporal sequences of patterns with state-dependent synapses *J. Phys. A: Math. Gen.* **27** 5879–87
[9] Zertuche F and Waelbroeck H 1999 Discrete chaos *J. Phys. A: Math. Gen.* **32** 175–89
[10] Alekseev V M and Yakobson M V 1981 Symbolic dynamics and hyperbolic dynamical systems *Phys. Rep.* **75** 287–325
[11] Falcioni M, Mantica G, Pigolotti S and Vulpiani A 2003 Coarse-grained probabilistic automata mimicking chaotic systems *Phys. Rev. Lett.* **91** 044101
[12] Alicki R and Fannes M 1994 Defining quantum dynamical entropy *Lett. Math. Phys.* **32** 75–82
[13] Alicki R and Fannes M 2001 *Quantum Dynamical Systems* (Oxford: Oxford University Press)
[14] Alicki R, Andries J, Fannes M and Tuyls P 1996 An algebraic approach to the Kolmogorov–Sinai entropy *Rev. Math. Phys.* **8** 167
[15] Chernoff N 1992 Ergodic and statistical properties of piecewise linear hyperbolic automorphisms of the two-torus *J. Stat. Phys.* **69** 111–34
[16] Vaienti S 1992 Ergodic properties of the discontinuous sawtooth map *J. Stat. Phys.* **67** 251
[17] Percival I C and Vivaldi F 1987 A linear code for the sawtooth and cat maps *Physica* D **27** 373
[18] De Bièvre S 1998 Chaos, quantization and the classical limit on the torus *Proc. 14th Workshop on Geometrical Methods in Physics (Bialowieza, 1995)* (Miodowa: Polish Scientific Publisher PWN) (*Preprint* mp_arc 96-191)
[19] De Bièvre S 2001 Quantum chaos: a brief first visit *Contemp. Math.* **289** 161
[20] Reed M and Simon B 1972 *Methods of Modern Mathematical Physics: I. Functional Analysis* (New York: Academic)
[21] Araki H and Lieb E H 1970 Entropy inequalities *Commun. Math. Phys.* **18** 160–70